Electronic Supplementary Material (ESI) for RSC Advances.


# Supporting Information

## Highly selective fluorescent turn-on –off sensing of $OH^-$, $Al^{3+}$and $Fe^{3+}$ ions by tuning ESIPT in metal organic framework and mitochondria targeted bio-imaging

Soumya Bhowal[a]*, Arijit Ghosh [b]*

# Table of content

28) **UV-VIS titration of Ligand with $OH^-$**
29) **PL titration of Ligand with $OH^-$**
30) **Titration of the $Al^{3+}$@MOF with $Fe^{3+}$ ion solution**
31) **Titration of the $Fe^{3+}$@MOF with $Al^{3+}$ ion solution**
32) **Fluorescence Intensity of the MOF in presence of $Al^{3+}$ and calculation of LOD**
33) **Fluorescence Intensity of the MOF in presence of $Fe^{3+}$ and calculation of LOD**
34) **Fluorescence Intensity of the MOF in presence of $OH^-$ and calculation of LOD**
35) **Recyclability of the MOF for $Al^{3+}$, $Fe^{3+}$, $OH^-$ ions**
36) **Time dependent photoluminescence**
37) **Zeta potential of MOF in presence of pH solutions and $OH^-$ ions**
38) **EDX of MOF recovered from metal ion solution of MOF.**

# 1. Experimental

## Ligand and MOF synthesis

### Synthesis of ligand

The synthesis of the 4, 8-dihydroxynaphthalene-2, 6-dicarboxylic acid was obtained in two steps. The first step involved the synthesis of disulpho derivative with sulphonation and the second step involves solid state hydroxylation.

### Synthesis of 4, 8-disulfonaphthalene-2, 6-dicarboxylic acid

In a 100 mL round bottom flask 1g of naphthalene-2, 6-dicarboxylic acid was taken and 5 mL of Oleum ($SO_3$, 65 wt%) was added to it. The solution is stirred at around 140$^{o}$C for 24 hours. The resulting solution was then cooled to room temperature and added to 50 mL of cold water in a drop wise manner. Acidity of the solution was balanced with $Na_2CO_3$ solution. A white precipitate formed which was then filtered and washed with water to remove excess acid from the surface of the precipitate. Thus 4, 8-disulfonaphthalene-2, 6-dicarboxylic acid is synthesized. FT-IR (KBr, $cm^{-1}$): 3596 (br), 2991 (br), 1693 (s), 1623 (w), 1604 (m), 1485 (w), 1427 (s), 1290 (s), 1193 (br), 1130 (br), 1047 (s), 908 (m), 803 (ss), 771 (ss), 738 (ss), 638 (s), 615 (s), 526 (w), 424 (w). 1H-NMR (500 MHz, $D_6$-DMSO): δ 8.48 (s, 2H), δ 9.604 (s, 2H), δ 13.126 (w, 2H).

### Synthesis of 4, 8-dihydroxynaphthalene-2, 6-dicarboxylic acid

0.5 g of 4, 8-disulfonaphthalene-2, 6-dicarboxylic acid and 0.25 g NaOH was mixed, dried and then sealed in a vacuumed glass tube for heating. The sealed tube then placed inside a furnace and heated around 320$^{0}$C for 2h with a heating rate 6$^{0}$C/min. After the heating was completed the tube was then brought into room temperature and cut open. The mixture was then dissolved in water and neutralised with diluted HCl solutions. A light yellow colour precipitate formed which was then washed, dried and collected. FT-IR (KBr, $cm^{-1}$): 3586 (br), 3479 (br), 3135 (br), 2917 (w), 1729 (s), 1610 (w), 1416 (w), 1266 (w), 1178 (ss), 1053 (s), 916 (w), 751 (w), 734 (w), 691 (w), 622 (m). 1H-NMR (500 MHz, $D_6$-DMSO): δ 7.414 (s, 2H), δ 8.296 (s, 2H), δ 10.690 (s, 2H).

**Synthesis of Zn-4, 8-dihydroxynaphthalene-2, 6-dicarboxylate MOF**

In a glass based scintillation vial $Zn(NO_3)_2.6H_2O$ (0.03 g, 0.1 mM ) and 4, 8-dihydroxynaphthalene-2, 6-dicarboxylic acid (0.025 g, 0.1 mM ) were taken. The reactants were dissolved in 3 mL DMF and 2 mL ethanol solvent mixture. The mixture is then dissolved with sonication and sealed tightly with teflon tape. Then the mixture is heated at $80^0$C for 12 hours in an oven. An orange colour cubic crystal generated at the bottom of the glass. The crystals were filtered and washed with DMF. FT-IR (KBr, $cm^{-1}$): 3467 (br), 3104 (br), 2804 (br), 1616 (s), 1585 (m), 1404 (s), 1353 (m), 1191 (ss), 1053 (s), 791 (s), 772 (m), 628 (s).

**Activation**

The activation method consisted of a two-step procedure to vacate the pores of the MOF from solvents and moisture. First the MOF was treated with dichloromethane (DCM) to replace the trapped high temperature boiling DMF and ethanol with a low temperature boiling DCM solvents. The MOF was then filtered from the DCM solvent and collected. The MOF was then heated and vacuumed at $80^0$C for 24 hours. The resulting activated MOF was used for further experiments.

**Material**

All the starting materials were of reagent grade and used as received from the commercial suppliers without any further purification. Powder XRD (PXRD) of the as-synthesised and activated MOF and MOF in different solutions were collected in Bruker D8 ADVANCE using Cu-Kα (λ = 1.5406 Å) in a 2θ range 5-$50^0$C. FTIR data of the MOF and ligand was obtained with PerkinElmer Spectrochem 100 FTIR spectrometer. High-resolution mass spectrometry (HRMS) of the ligands was collected on QTOF−Micro YA 263 mass spectrometer in negative ESI mode. Fluorescence emission studies were performed using a HORIBA JOBIN YVON Fluoromax-4 spectrofluorometer. UV-Visible spectra data were collected in Perkin-Elmer Lambda 950 UV/vis instrument. Thermo gravimetric analyses of the As-synthesized and activated MOF were collected with TA Instrument SDT Q600 at a 5 °C/min heating and 100 mL/min flow rate under $N_2$ atmosphere. TCSPC measurements were obtained in an IBH Fluorocube by exciting with Picoseconds diode laser (IBH Nanoled-07). JEOL JEM 2010 high-resolution microscope instrument is used for TEM images. Dynamic

light scattering (DLS) and Zeta potential of the solutions were obtained using NanoZS90 (Malvern) instrument using Millipore water as solvents.

**Live-cell confocal microscopy**

Live-cell imaging was carried out using confocal laser-scanning microscope (Leica TCS SP8) with a UV-laser and 63X/1.4 NA oil objective equipped with a heated environmental chamber set to 37º C with optimal $CO_2$ facility. Briefly, MCF7 cells seeded on cover glass bottom dish (Genetix, Biotech Asia Pvt. Ltd.) were incubated with the MOF at pH-7 and pH-9 separately for 3 hours before imaging. Nuclei were subsequently stained with Hoechst 33342 (Blue) (Invitrogen). This was followed by live cell confocal microscopy. Images were collected and processed using the Leica software and sized in Adobe Photoshop 7.0.

**Cell Survival Assay**

MCF7 cells (6 x $10^3$) were seeded in 96-well plates (BD Biosciences, USA) and treated with the MOF at pH-7 and pH-9 separately at the indicated concentrations. After 72-h treatment, cell survival was assessed by 3-(4, 5-dimethylthiazol-2-yl)-2, 5- diphenyltetrazolium bromide (MTT) assay. Briefly, cells were washed with 1X PBS and treated with MTT reagent (Sigma) for 3 h at 37º C and the resulting formazan was dissolved in 100 µL of Dimethyl Sulfoxide. Plates were analyzed on Molecular Devices SpectraMax M2 Microplate Reader at 570 nm. The percent inhibition of viability for each concentration of the compounds was calculated with respect to the control. Data represent mean values ± s.e.m. for three independent experiments.

## 2. HRMS of the ligand

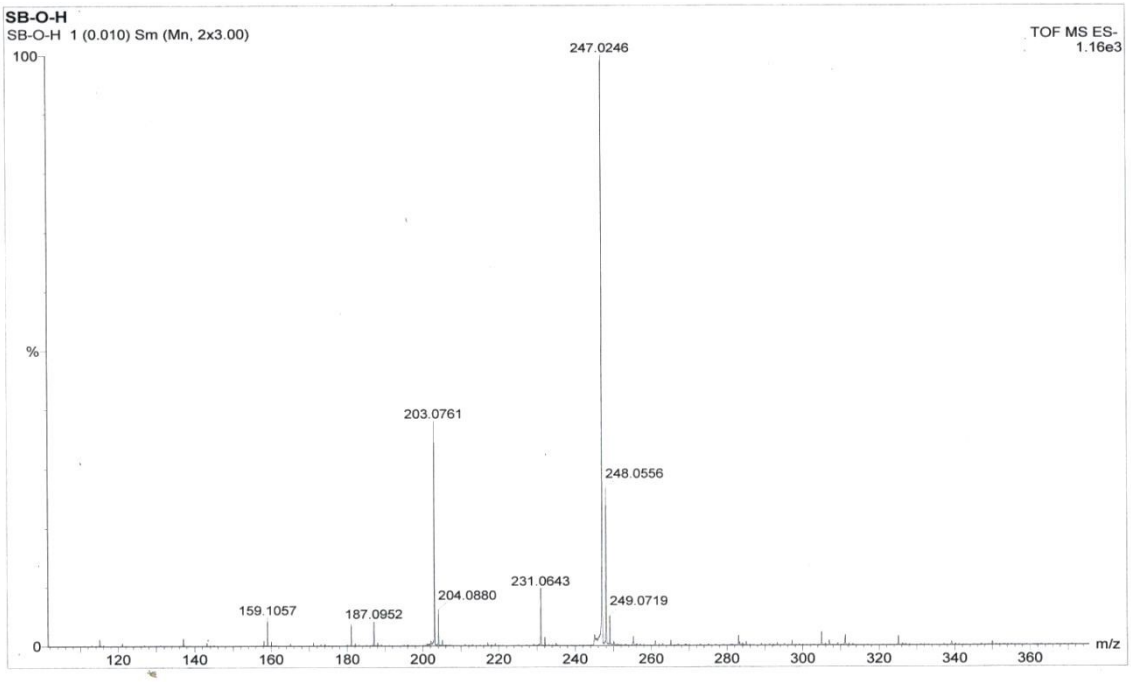


Figure 1S: The HRMS data of 4, 8-dihydroxynaphthalene-2, 6-dicarboxylic acid in ESI (-ve) mode.

## 3. NMR of the ligand

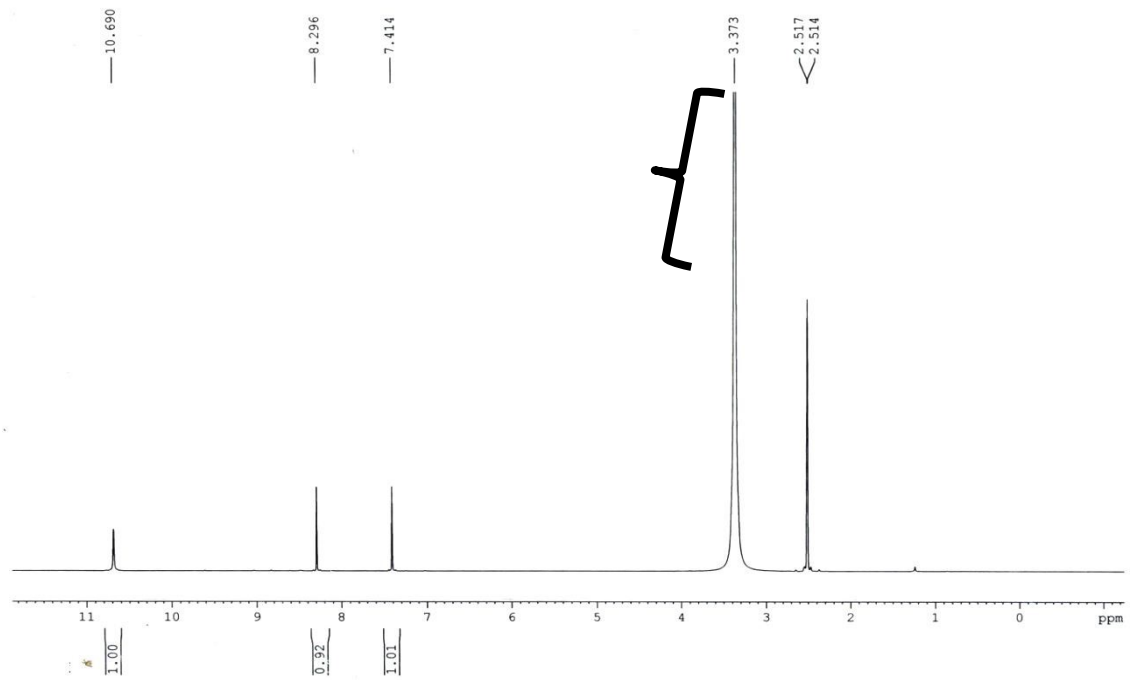


Figure 2S: The $^{1}H$ NMR of 4, 8-dihydroxynaphthalene-2, 6-dicarboxylic acid

## 4. Thermo gravimetric Analysis

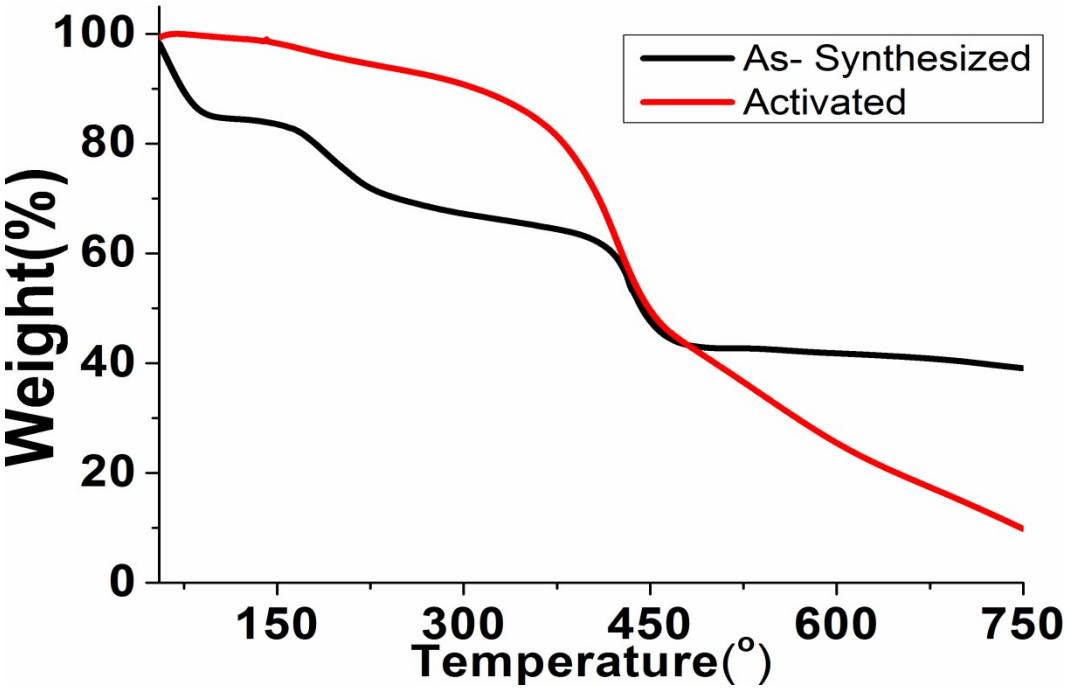


Figure 3S: Thermo gravimetric Analysis of as-synthesised and activated MOF

## 5. Fourier-transform infrared spectroscopy

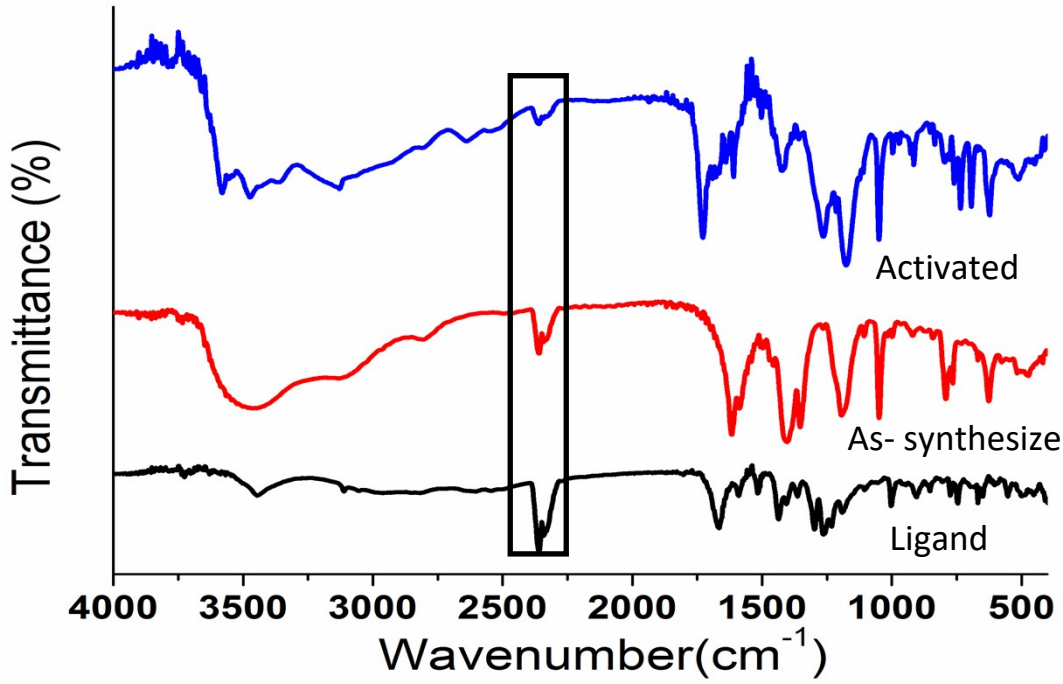


Figure 4S: The FTIR of Activated MOF, as-synthesized MOF and ligand. The black marked peak represents the C-O stretching of atmospheric $CO_2$.

## 6. Transmission Electron Microscopy

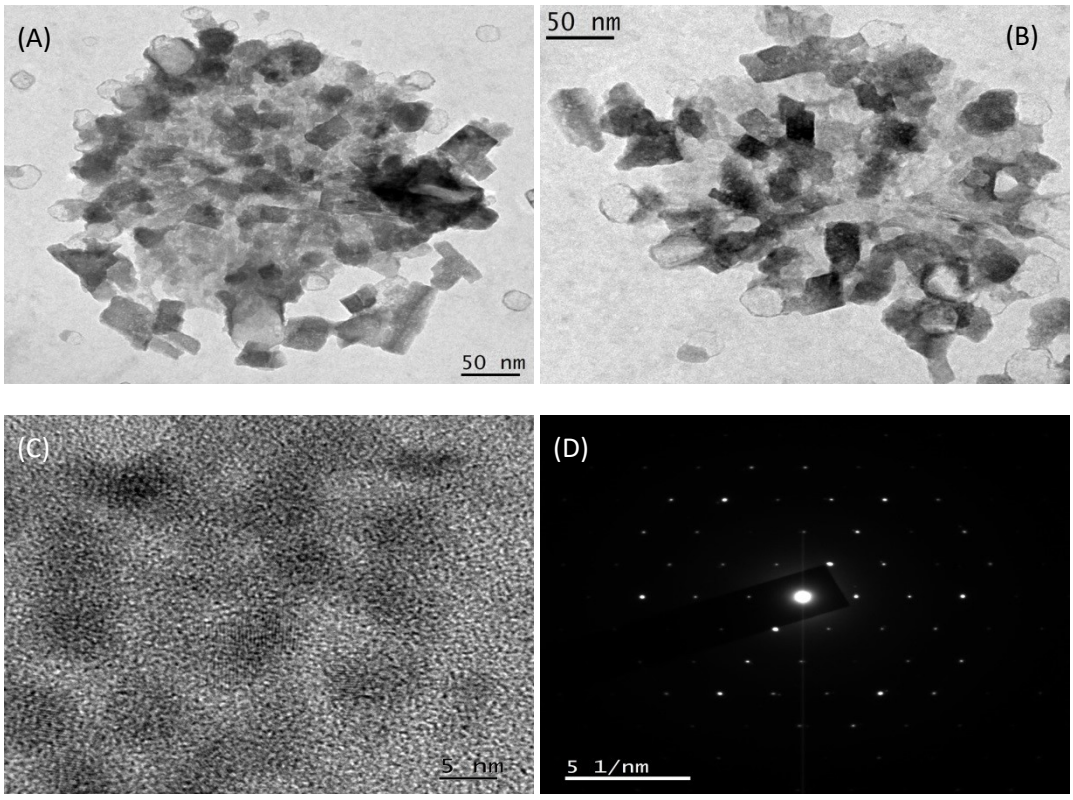

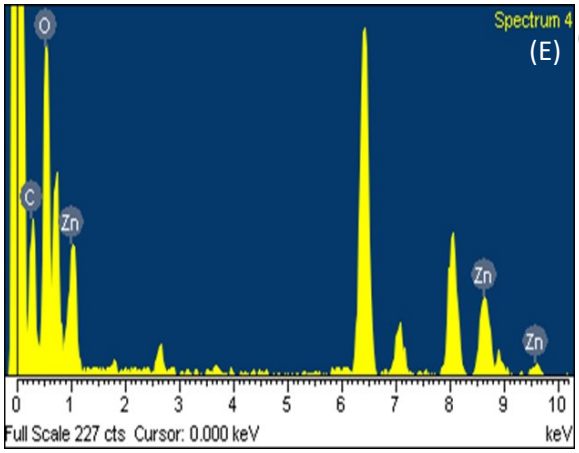


(F)

| Element | Weight% | Atomic% |
|---|---|---|
| C K | 15.12 | 30.38 |
| O K | 33.63 | 50.71 |
| Zn K | 51.25 | 18.91 |
| Totals | 100.00 | |

Figure 5S: Transmission electron microscopy of the MOF. (A), (B) represents the nano scale MOF particle. (C) Represents the HRTEM image. (D) Represents the SAED of the particles. (E), (F) Represents the EDX data and element analysis table.

## 7. Optical properties of the MOF

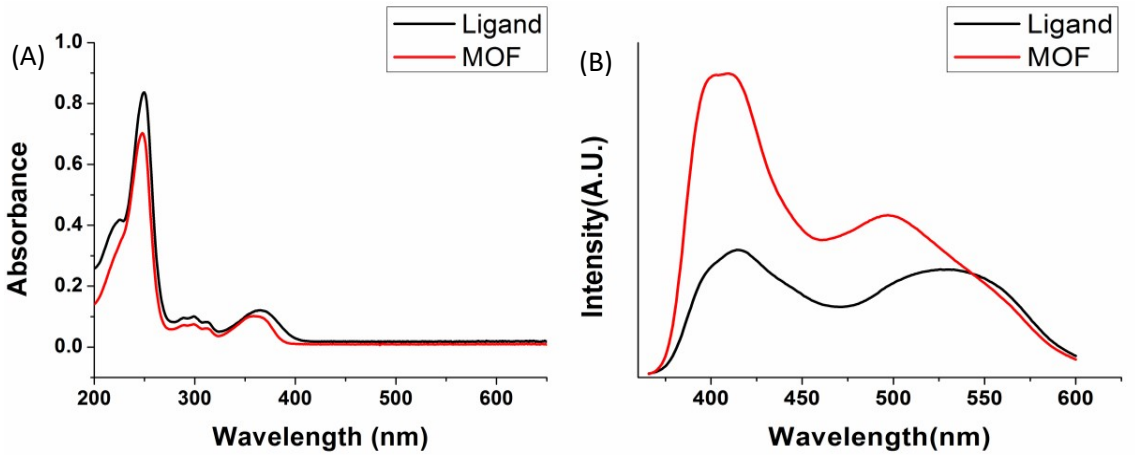

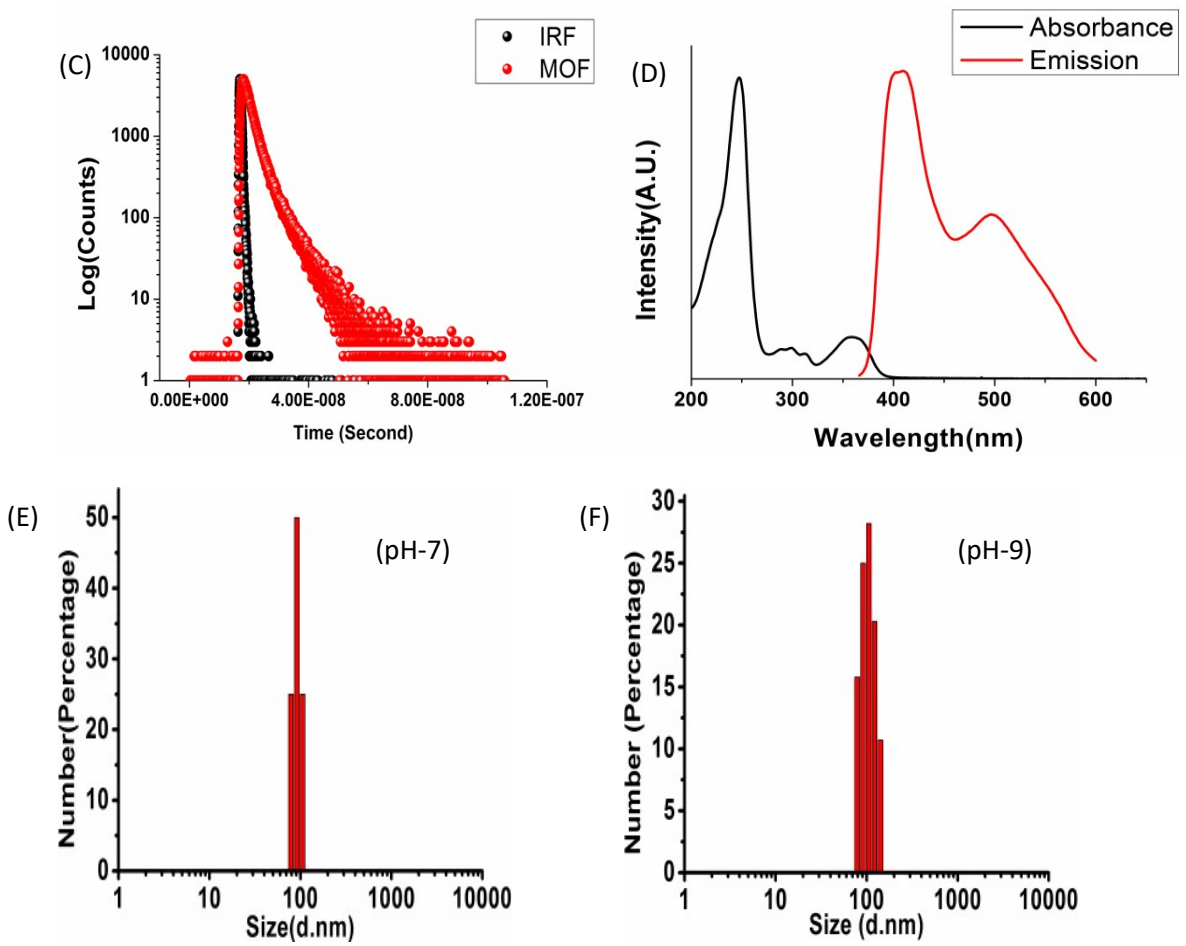


Figure 6S: represents the optical properties. (A) Represents the UV-VIS plots of ligand and MOF. (B) PL data of ligand and MOF. (C) Fluorescence decay (TCSPC) of the MOF. (D) Represents the UV-VIS and PL curve with a huge stocks shift. (E) DLS (hydrodynamic diameter) of the MOF in pH-7. (F) DLS (hydrodynamic diameter) of the MOF in pH-9.

## 8. pH titrations of Ligand and MOF

(A)

(B)

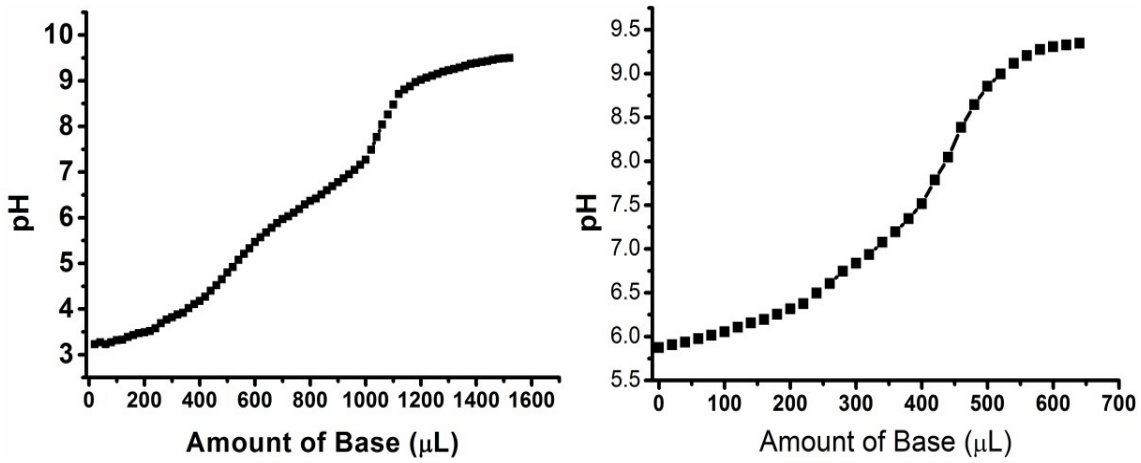


Figure 7S: Base vs pH titration of ligand and MOF. (A) The titration of ligand. (B) The titration of MOF.

## 9. NaOH and HCl vs Emission titration

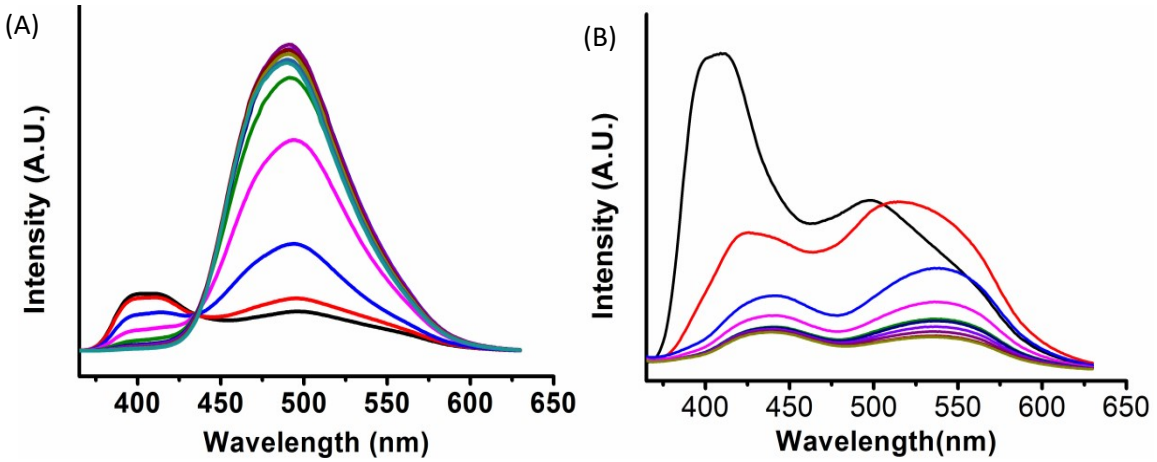


Figure 8S: Titration of MOF by acid and base.(A) Represents the PL titration of MOF with NaOH, (B) PL titration of MOF with HCl.

# 10. UV-VIS Titrations of the MOF by anions

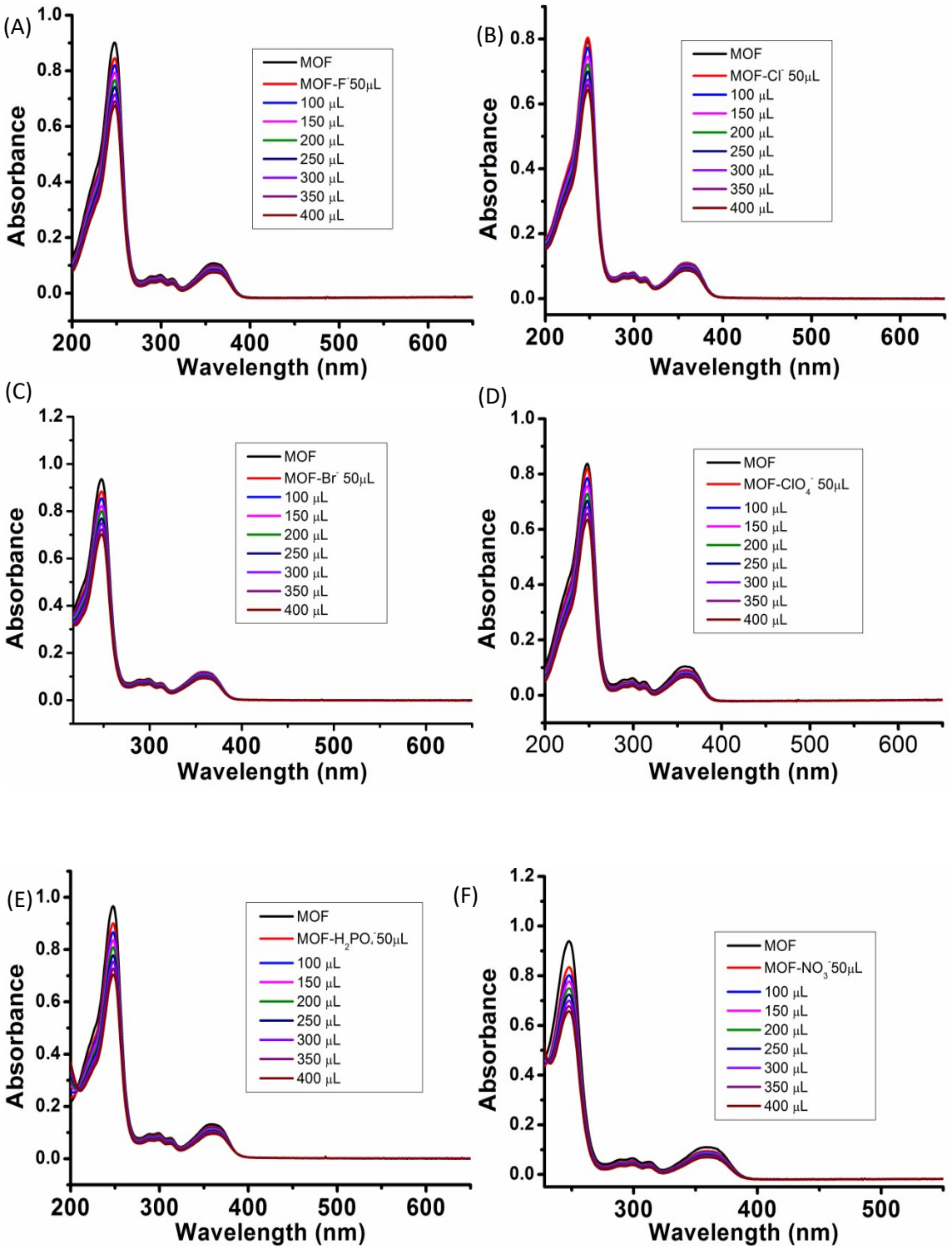

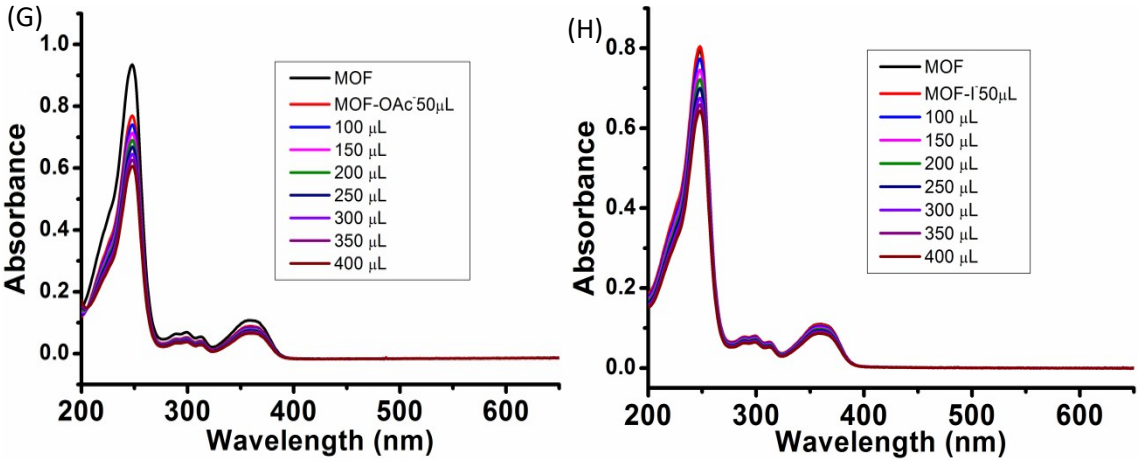


Figure 9S: The UV-VIS titration of the MOFs with (A) $F^-$, (B) $Cl^-$, (C) $Br^-$, (D) $ClO_4^-$, (E) $H_2PO_4^-$, (F) $NO_3^-$, (G) $OAc^-$,(H) $I^-$.

## 11. Effect on the UV-VIS of the MOF with addition of $OH^-$ in presence of other anions

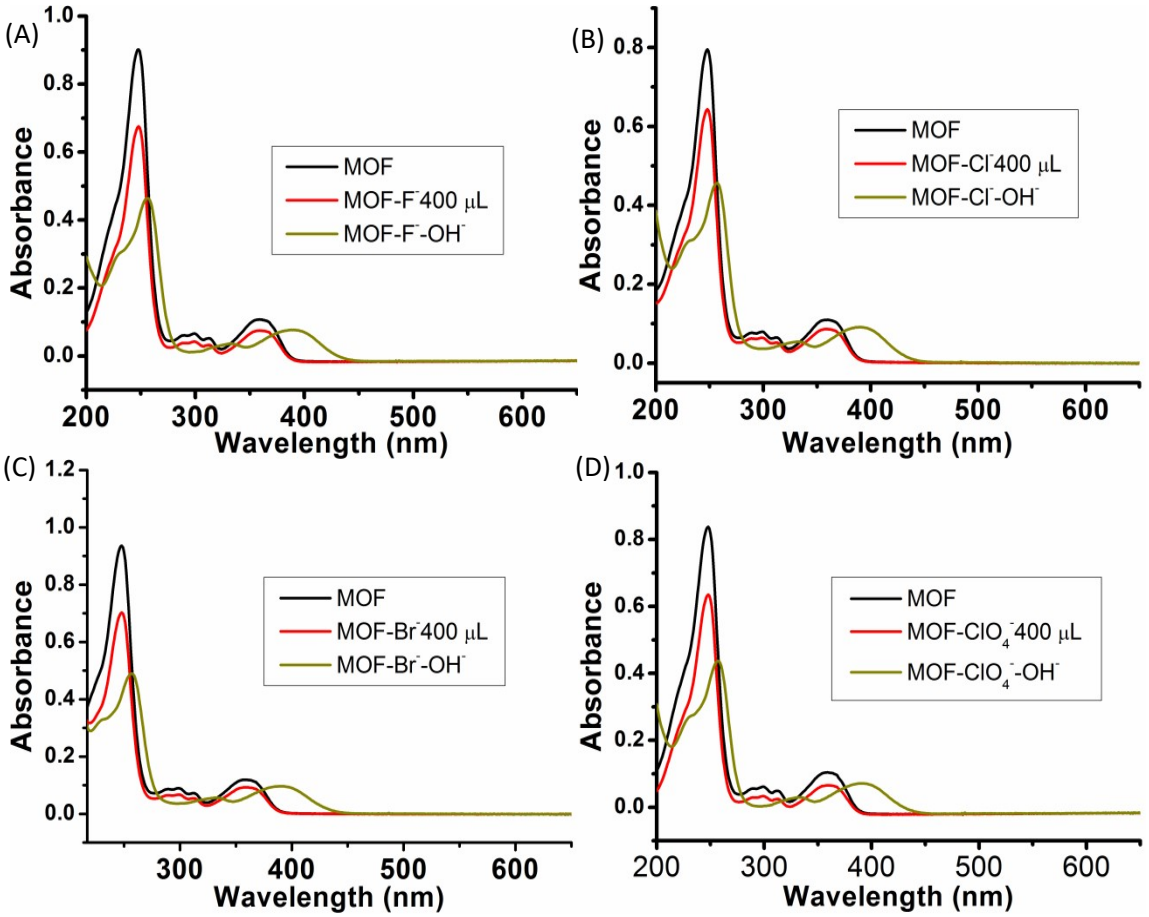

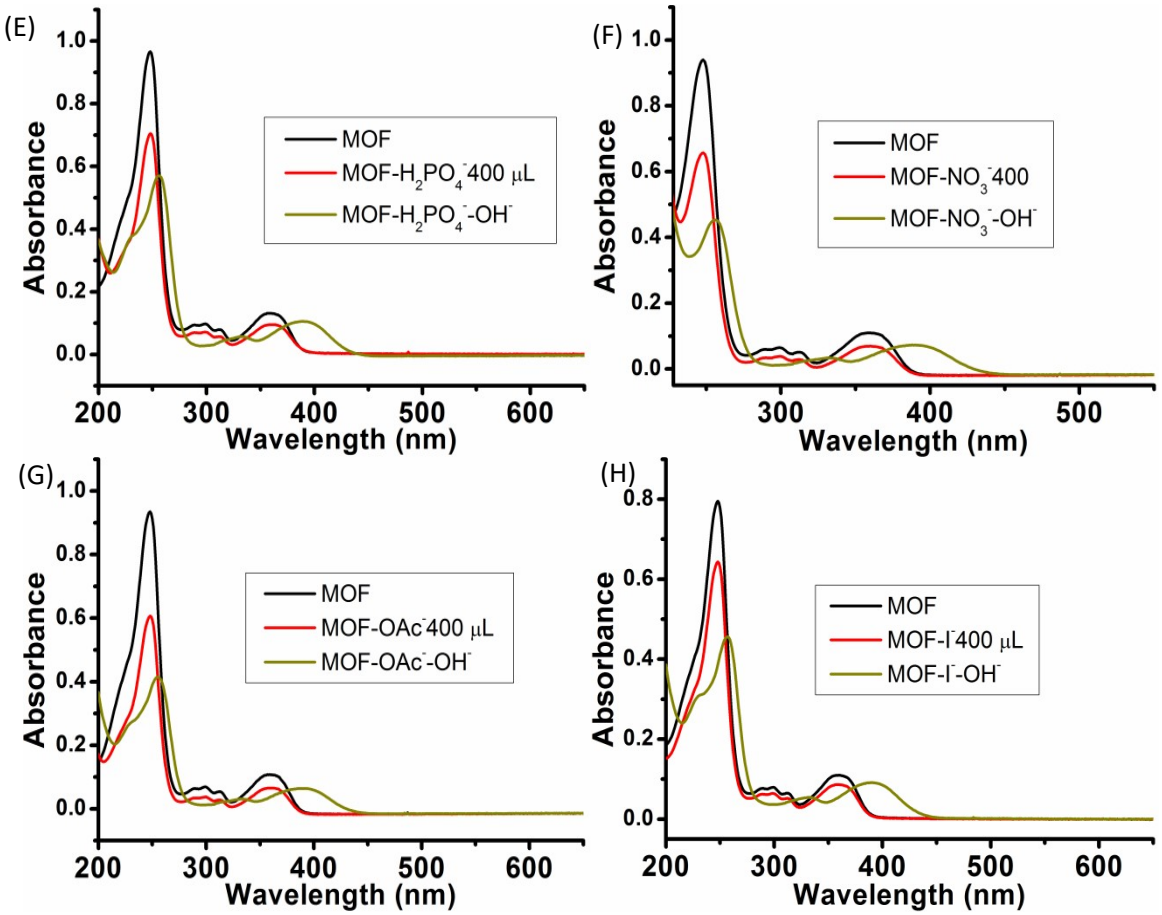


Figure 10S: Effect on UV-VIS curve nature of the MOF due to $OH^-$ addition in the MOF solution with other anions (A) $F^-$, (B) $Cl^-$, (C) $Br^-$, (D) $ClO_4^-$, (E) $H_2PO_4^-$, (F) $NO_3^-$, (G) $OAc^-$ ,(H) $I^-$.

## 12. PL Titrations of the MOF by anions

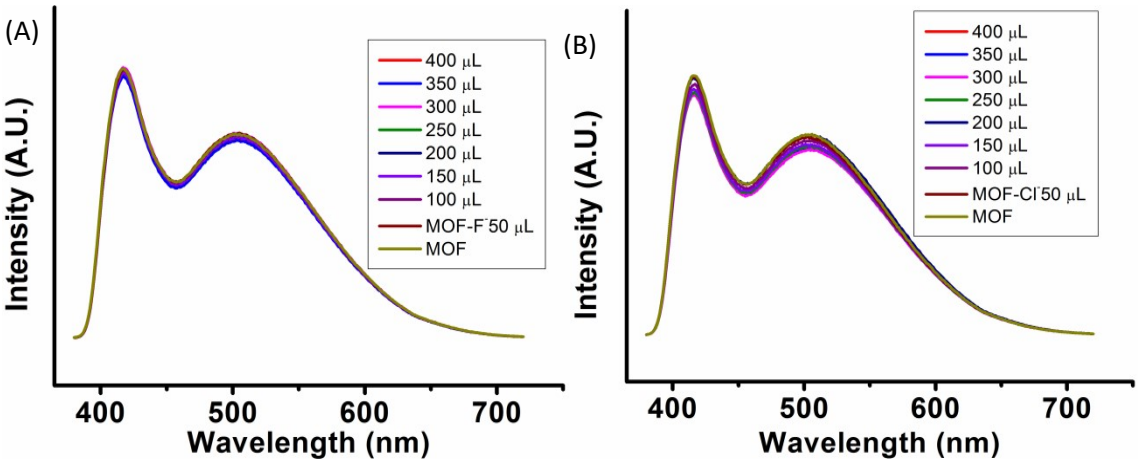

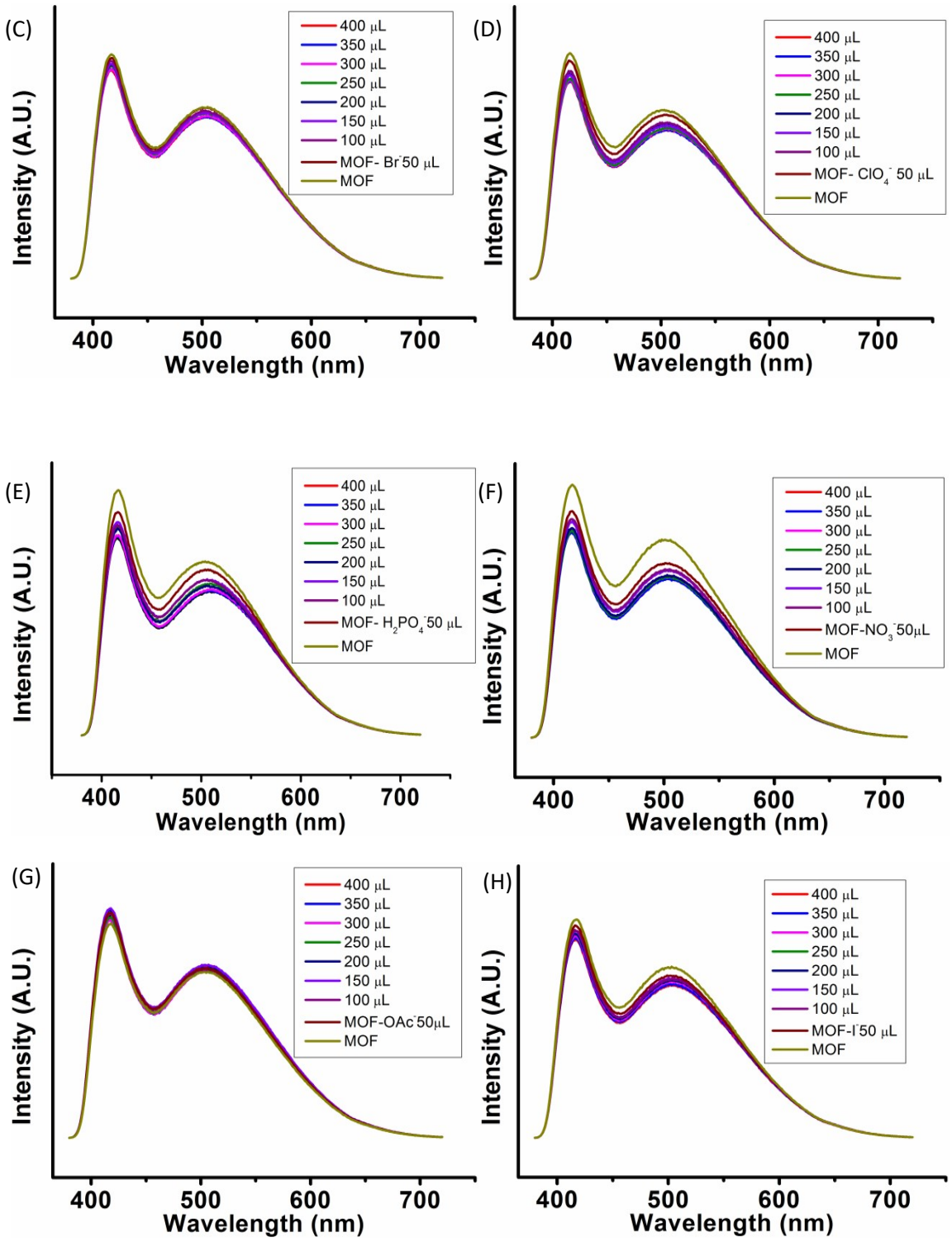


Figure 11S: The PL titration of the MOFs with (A) $F^-$, (B) $Cl^-$, (C) $Br^-$, (D) $ClO_4^-$, (E) $H_2PO_4^-$, (F) $NO_3^-$, (G) $OAc^-$,(H) $I^-$.

## 13. Effect on the PL of the MOF with addition of $OH^-$ in presence of other anions

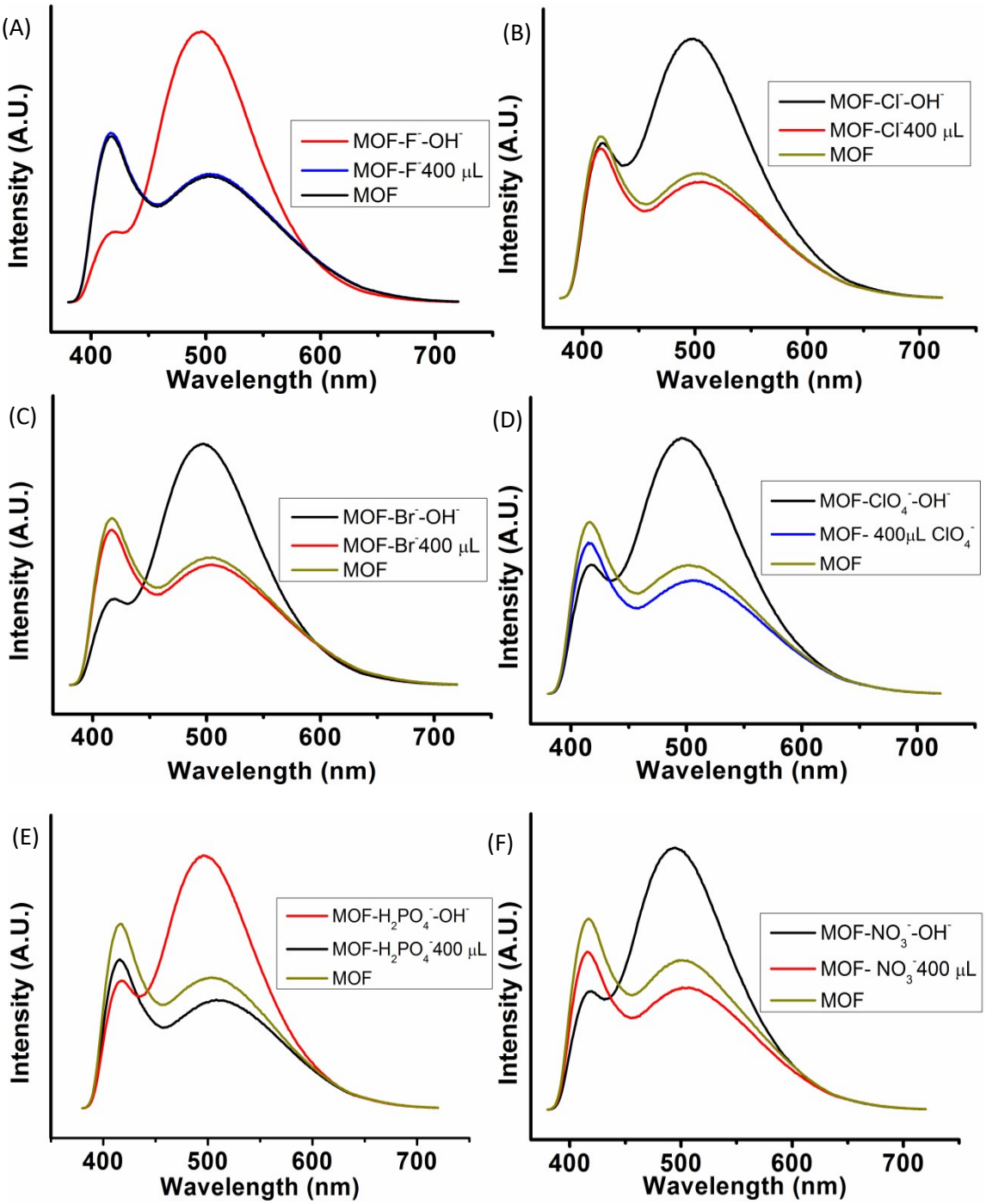

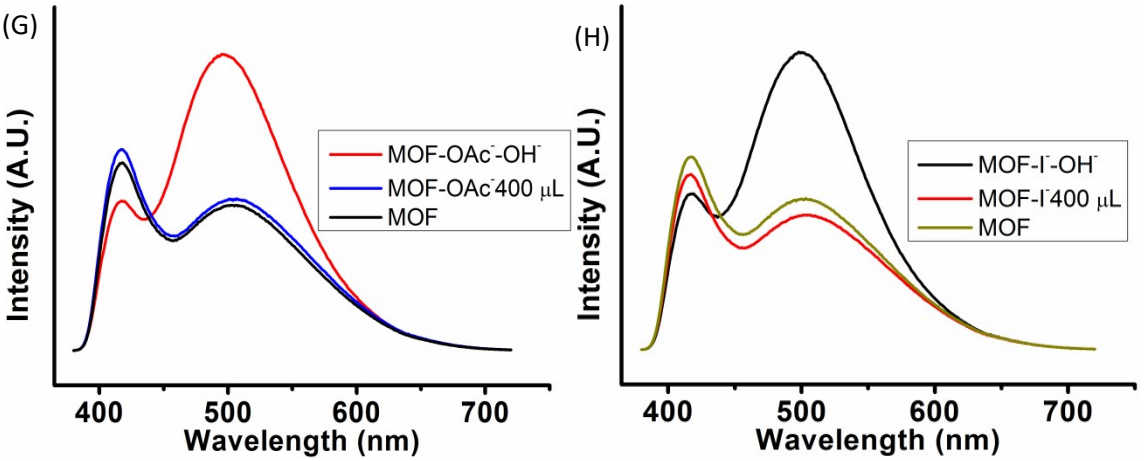


Figure 12S: Effect on PL curve nature of the MOF due to $OH^-$ addition in the MOF solution with other anions (A) $F^-$, (B) $Cl^-$, (C) $Br^-$, (D) $ClO_4^-$, (E) $H_2PO_4^-$, (F) $NO_3^-$, (G) $OAc^-$,(H) $I^-$.

## 14. Time-correlated Single Photon Counting of MOF in presence of $OH^-$ anion

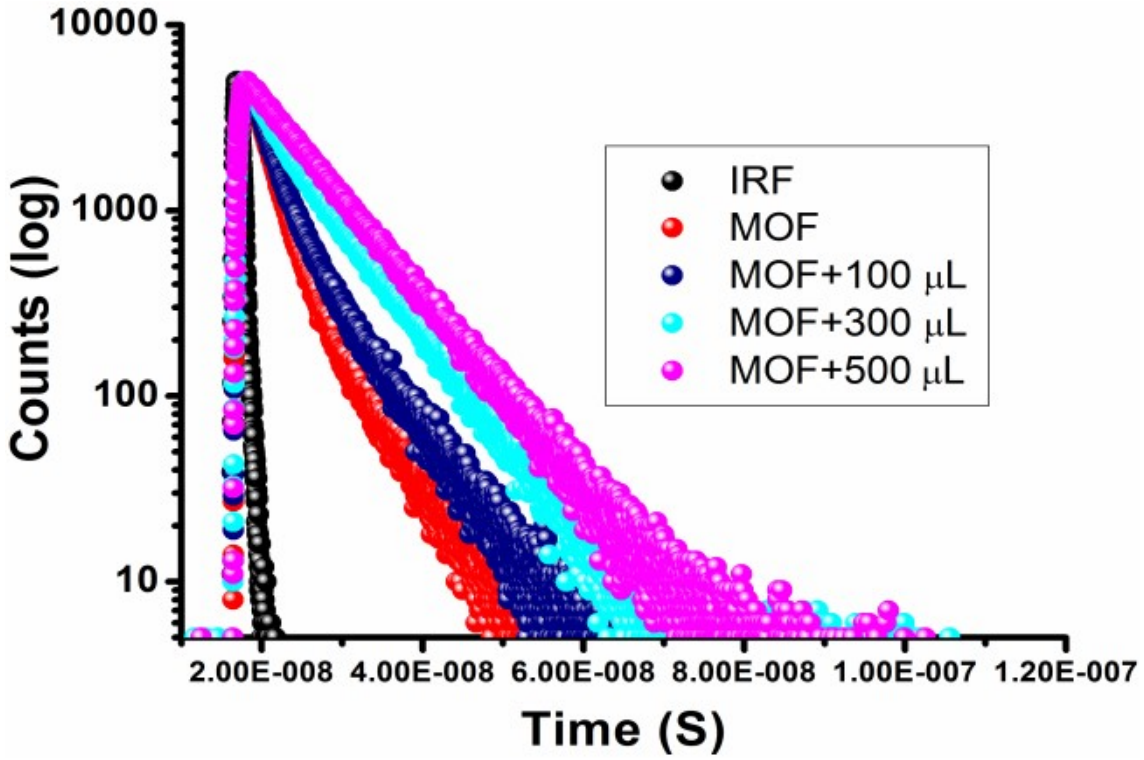


Figure 13S: The fluorescence decay of MOF and MOF solution with $OH^-$ anion

# 15. UV-VIS Titrations of MOF with Metal Ions

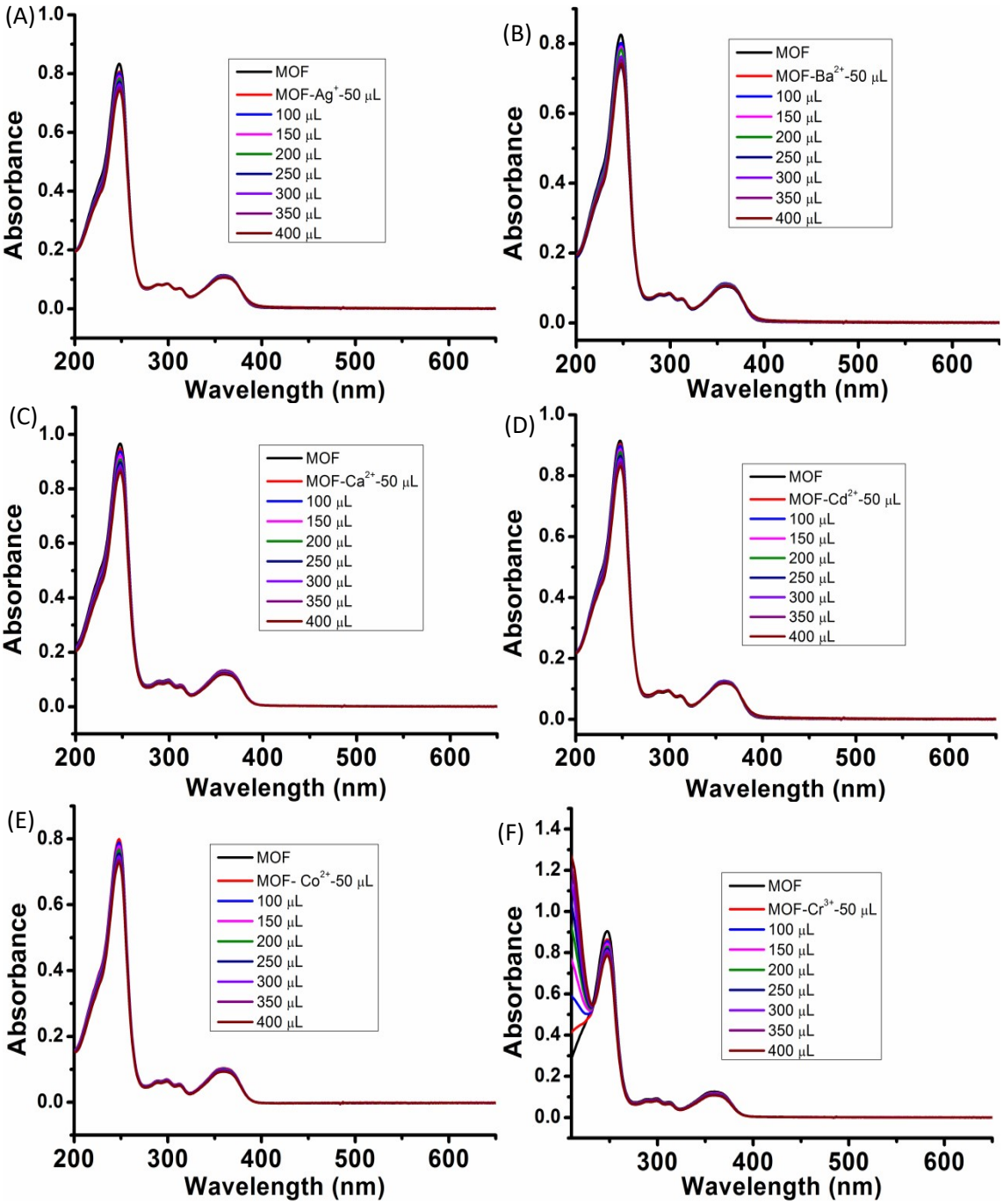

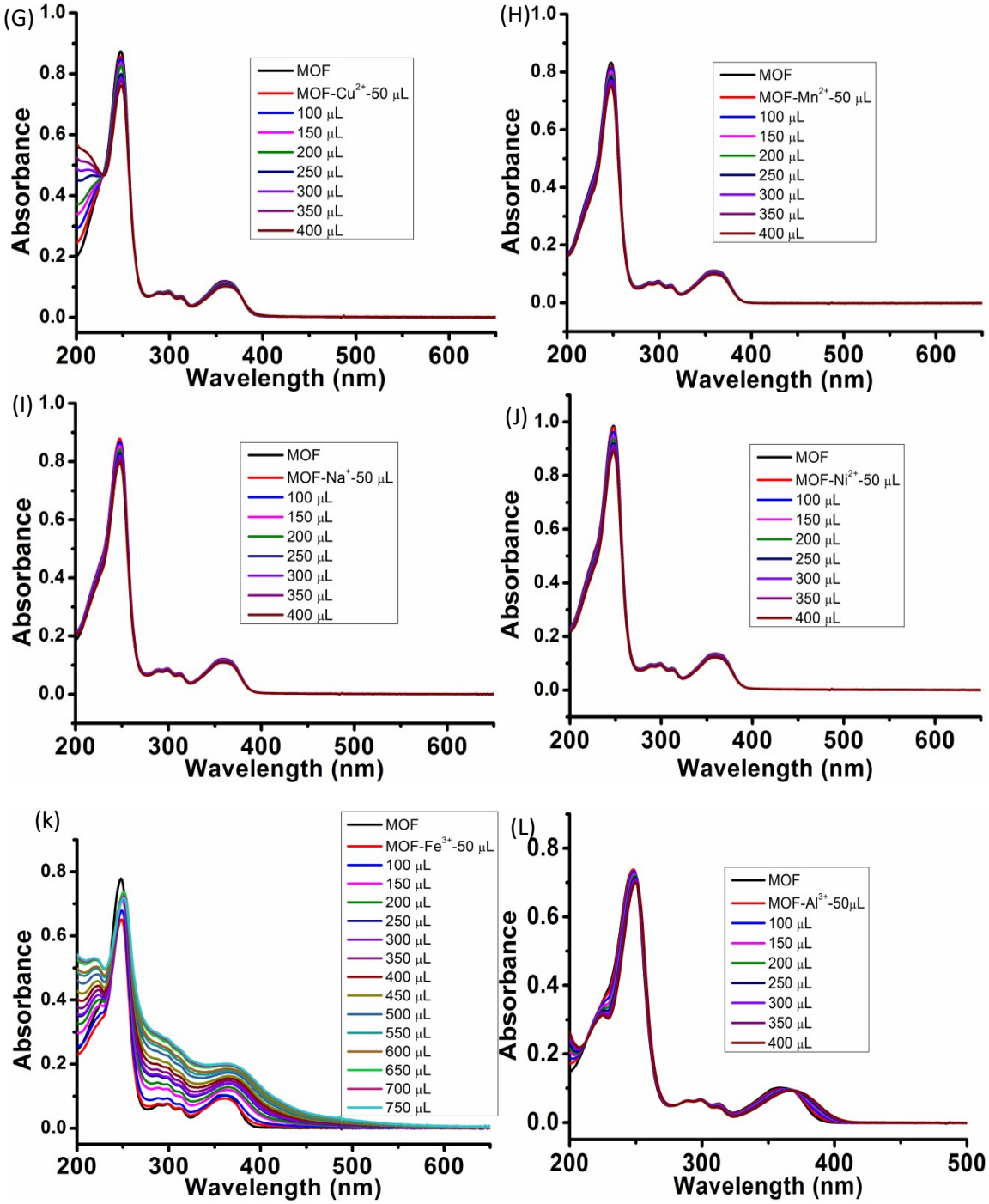


Figure 14S: UV-VIS titration of MOF in presence of metal ions (A) $Ag^{+}$, (B) $Ba^{2+}$, (C) $Ca^{2+}$, (D) $Cd^{2+}$, (E) $Co^{2+}$, (F) $Cr^{3+}$, (G) $Cu^{2+}$, (H) $Mn^{2+}$, (I) $Na^{+}$, (J) $Ni^{2+}$, (k) $Fe^{3+}$, (l) $Al^{3+}$

# 16. PL Titrations of MOF with Metal Ions

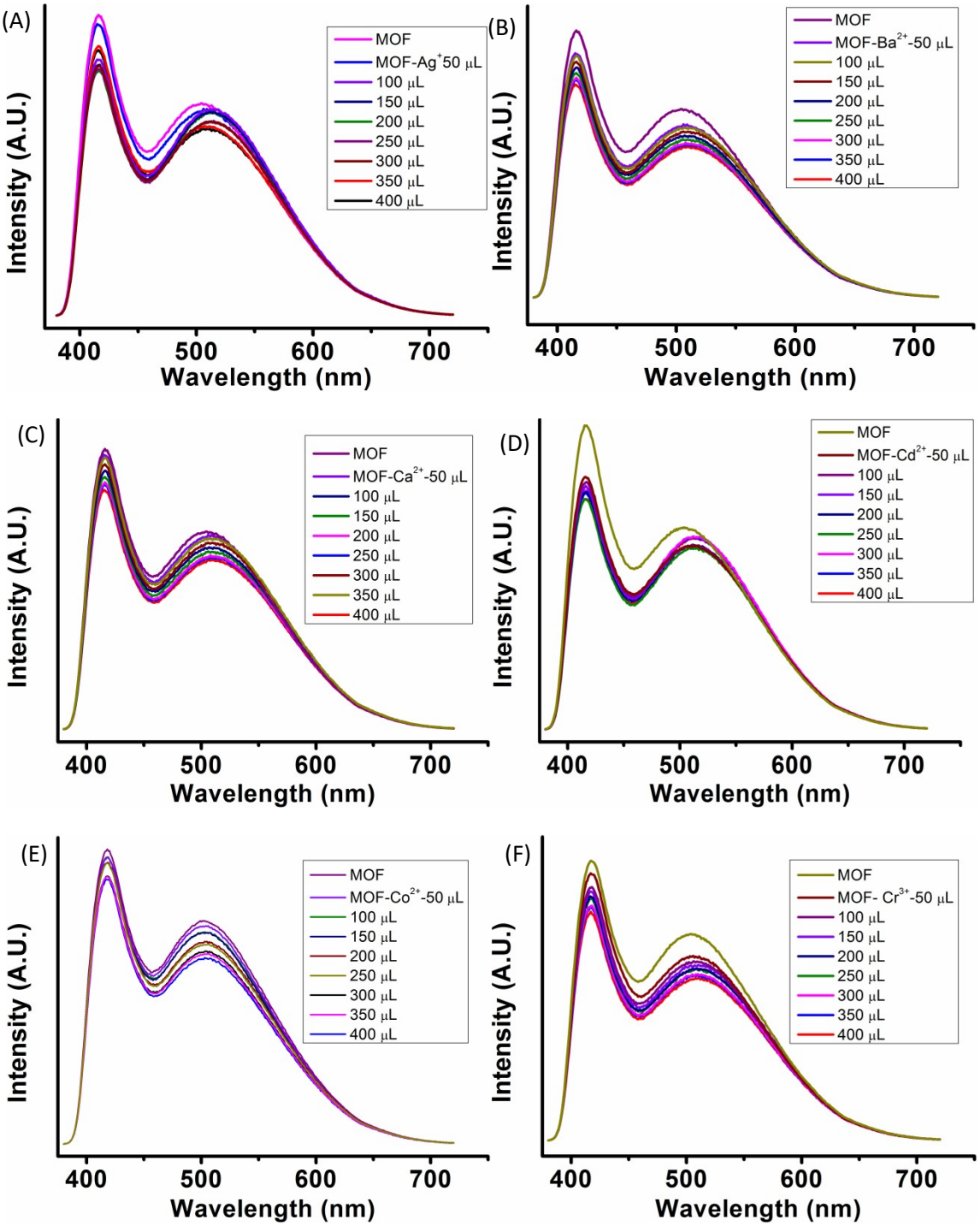

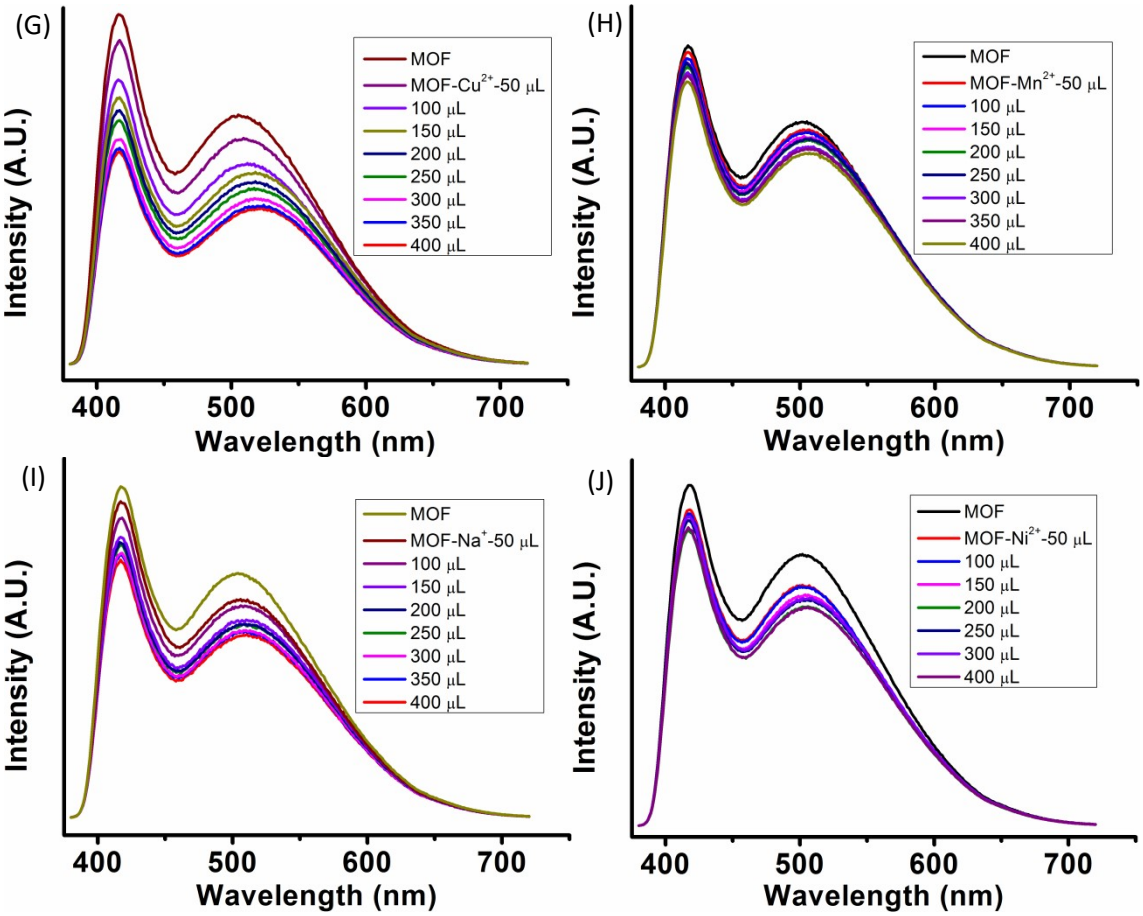


Figure 15S: The PL titration of MOF with metal ions (A) $Ag^{+}$, (B) $Ba^{2+}$, (C) $Ca^{2+}$, (D) $Cd^{2+}$, (E) $Co^{2+}$, (F) $Cr^{3+}$, (G) $Cu^{2+}$, (H) $Mn^{2+}$, (I) $Na^{+}$, (J) $Ni^{2+}$

17. **Effect on the UV-VIS of the MOF with addition of $Al^{3+}$ in presence of other Metal ions**

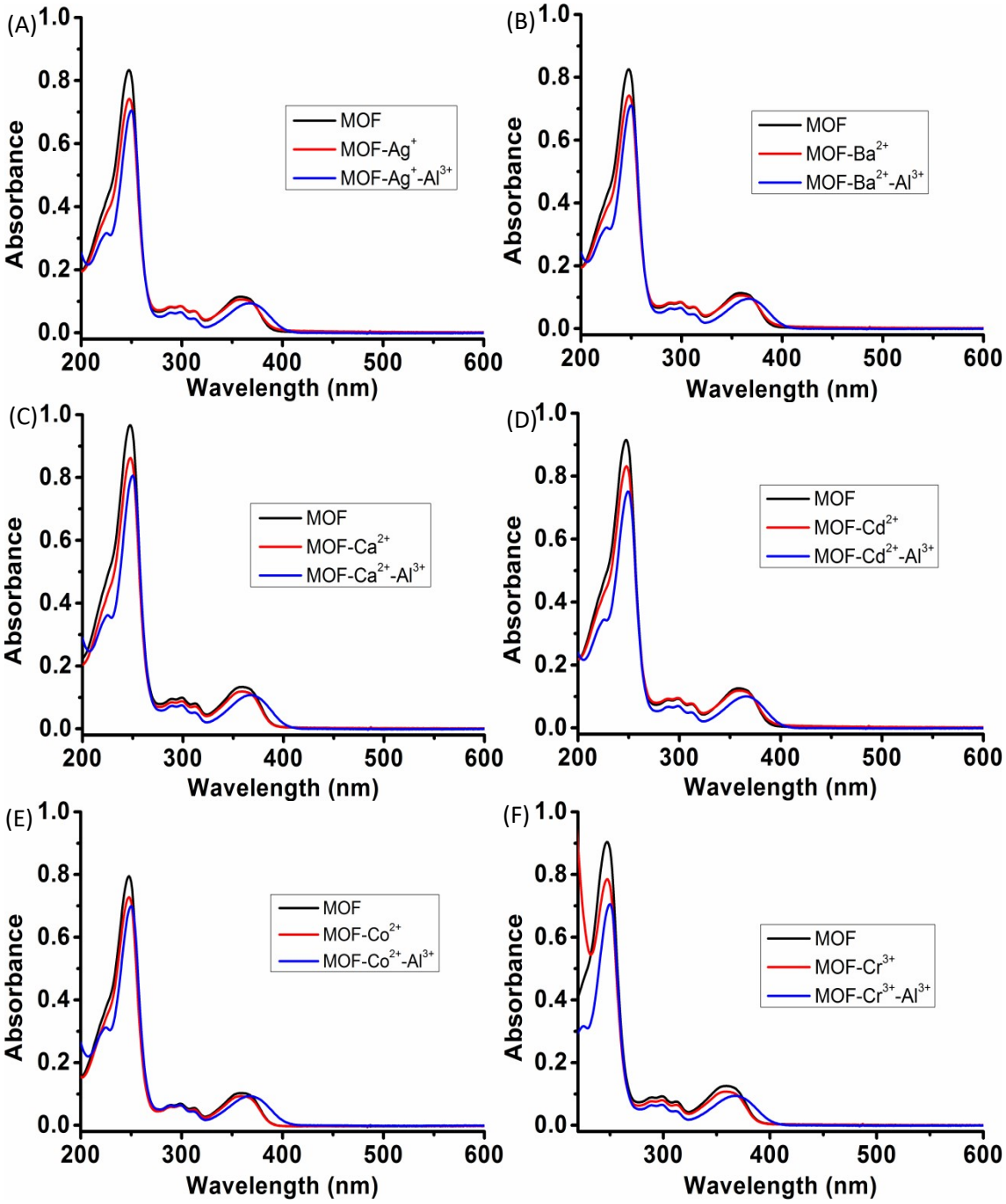

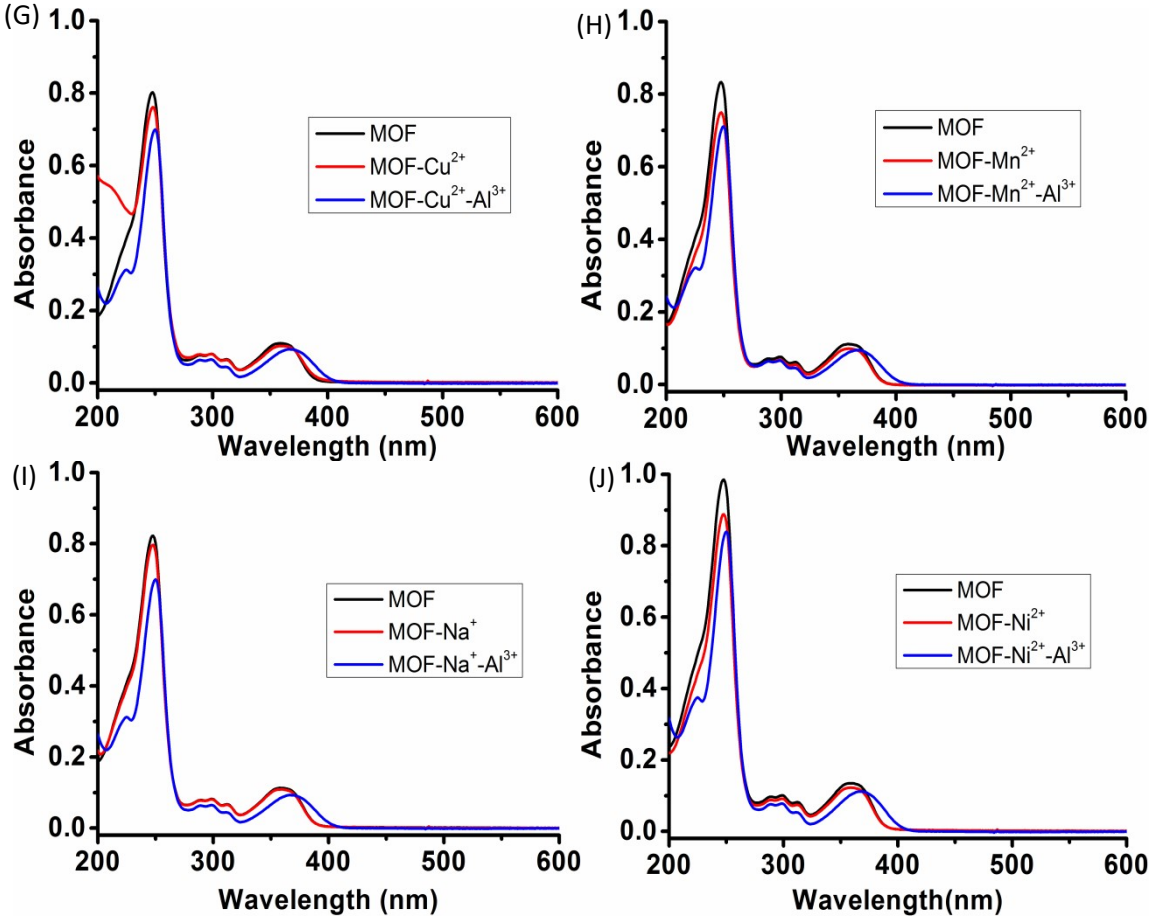


Figure 16S: Effect on UV-VIS curve nature of the MOF due to $Al^{3+}$ addition in the MOF solution with metal ions (A) $Ag^{+}$, (B) $Ba^{2+}$, (C) $Ca^{2+}$, (D) $Cd^{2+}$, (E) $Co^{2+}$, (F) $Cr^{3+}$, (G) $Cu^{2+}$, (H) $Mn^{2+}$, (I) $Na^{+}$, (J) $Ni^{2+}$

## 18. Effect on the PL of the MOF with addition of $Al^{3+}$ in presence of other Metal ions

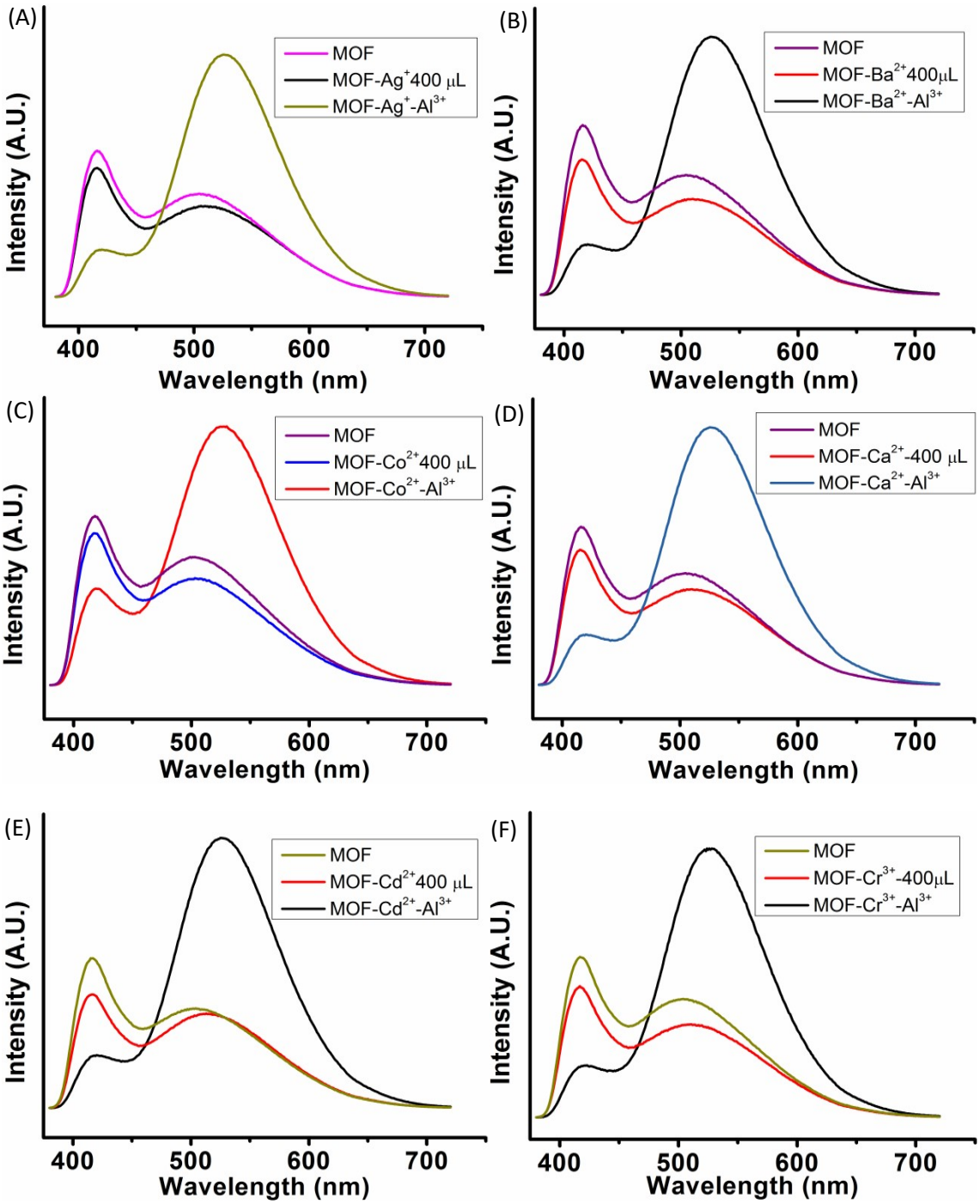

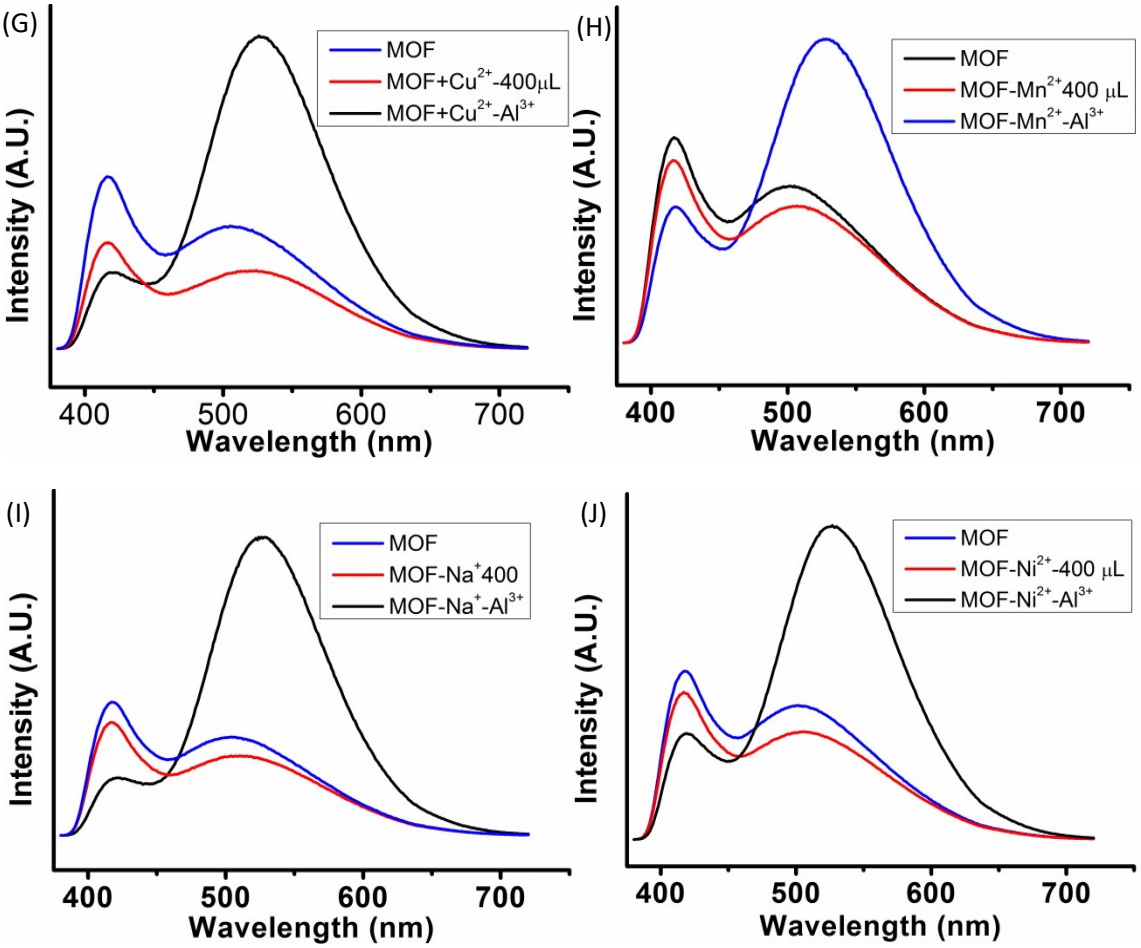


Figure 17S: Effect on PL curve nature of the MOF due to $Al^{3+}$ addition in the MOF solution with metal ions (A) $Ag^{+}$, (B) $Ba^{2+}$, (C) $Ca^{2+}$, (D) $Cd^{2+}$, (E) $Co^{2+}$, (F) $Cr^{3+}$, (G) $Cu^{2+}$, (H) $Mn^{2+}$, (I) $Na^{+}$, (J) $Ni^{2+}$

## 19. Time-correlated Single Photon Counting of MOF in presence of $Al^{3+}$ ion

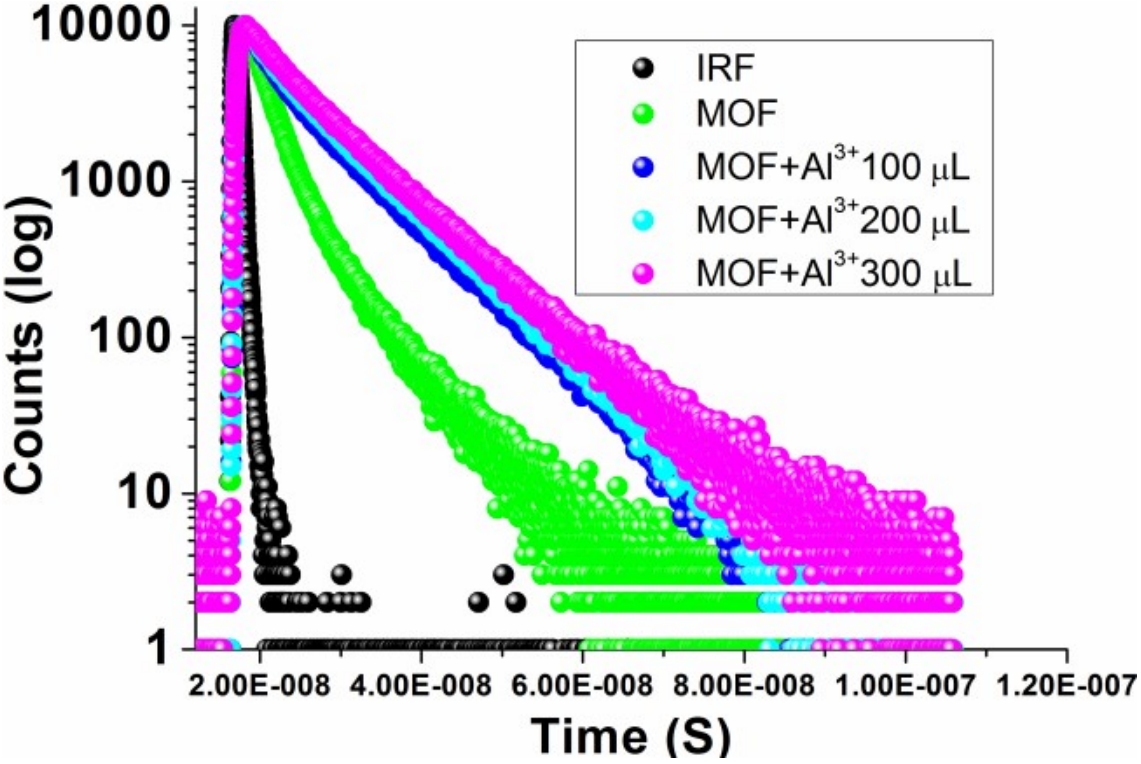


Figure 18S: The fluorescence decay of MOF and MOF solution with $Al^{3+}$ metal ion.

## 20. Dynamic light scattering (particle size) of the MOF in presence $Al^{3+}$ ions

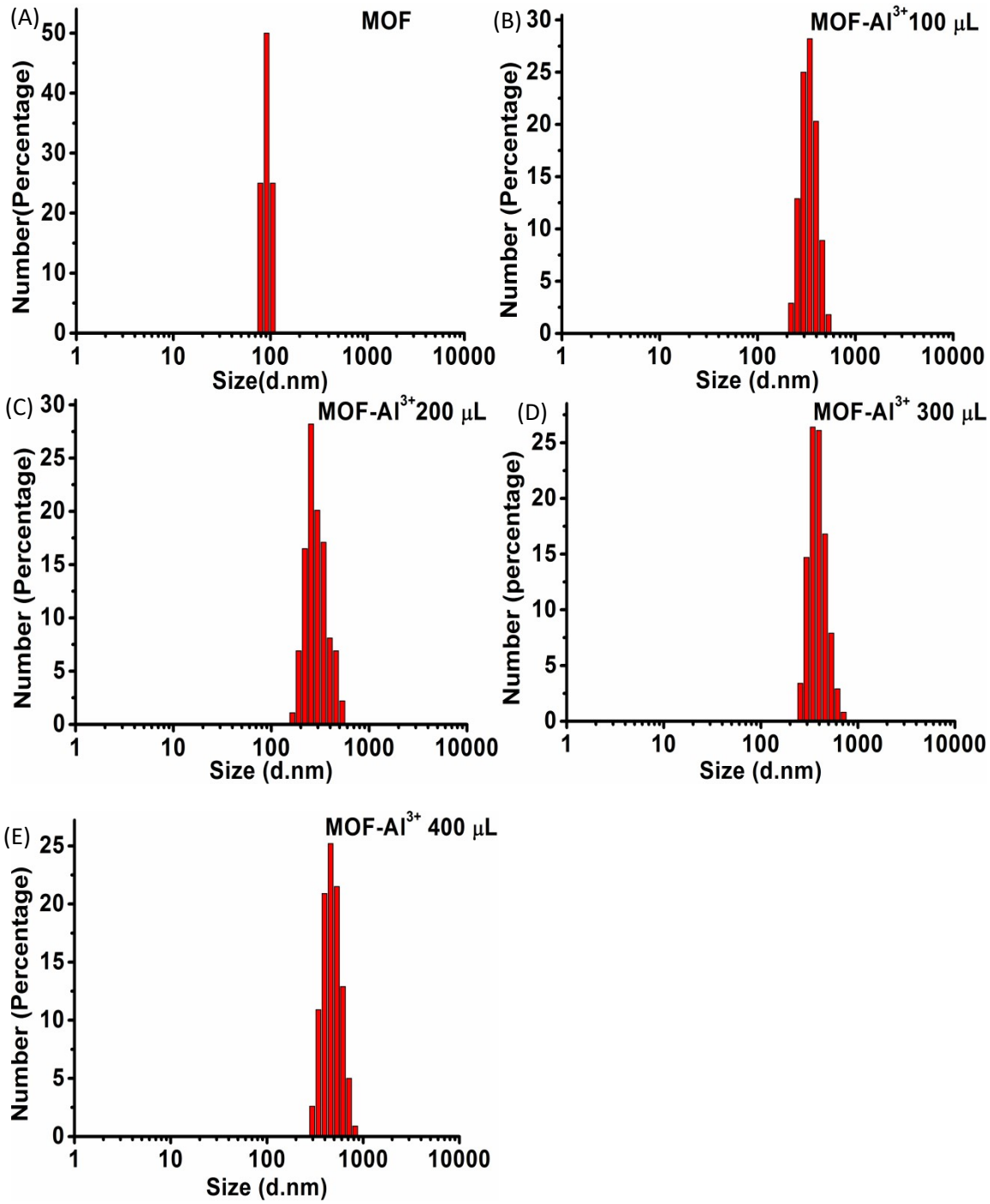


Figure 19S: The particle Size (DLS) of the MOF and MOF in presence of $Al^{3+}$ metal ion

## 21. Zeta potential of the MOF in presence of $Al^{3+}$ ions

**MOF**

(A)

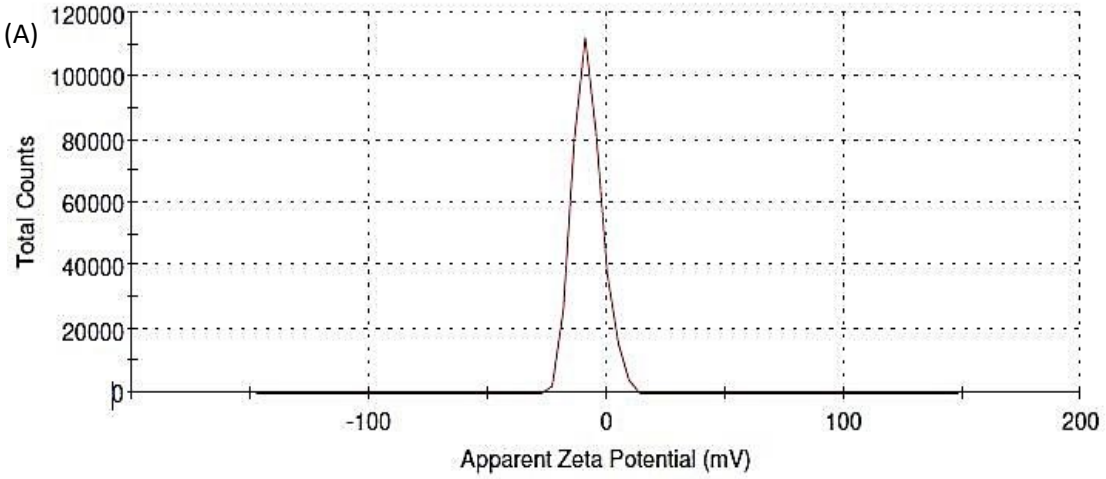


**M**

**OF-$Al^{3+}$ 100 µL**

(B)

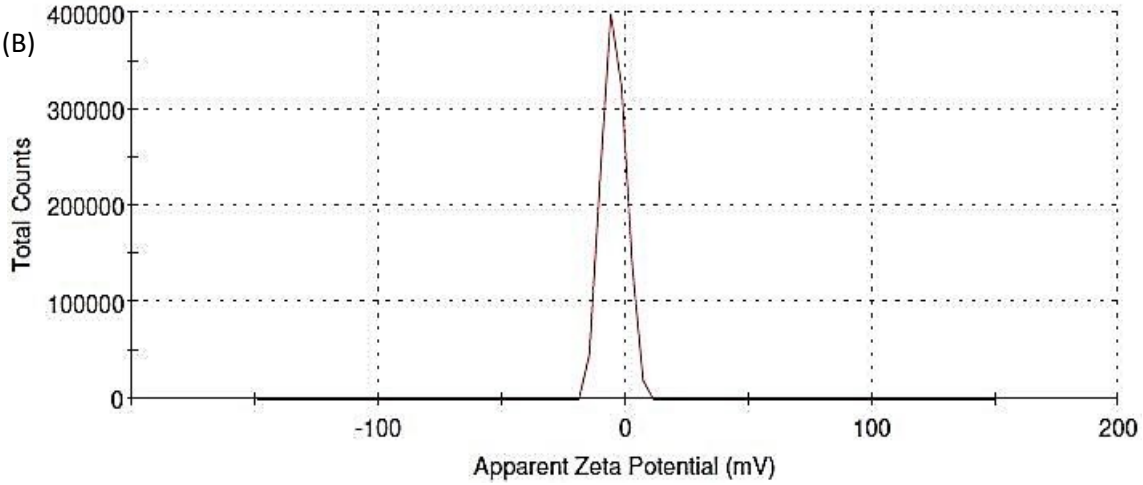


**MOF-$Al^{3+}$ 200 µL**

(C)

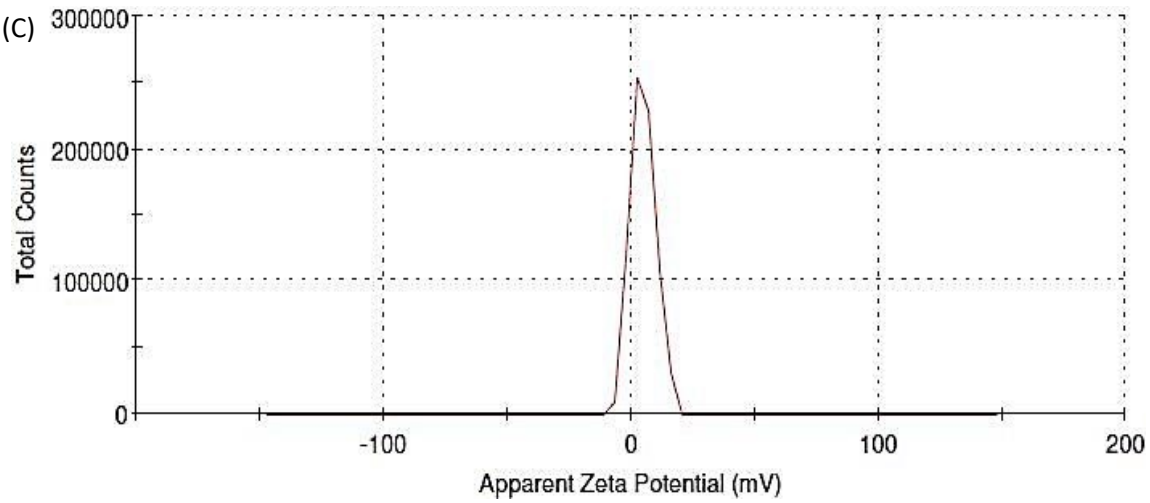

## MOF-$Al^{3+}$ 300 µL

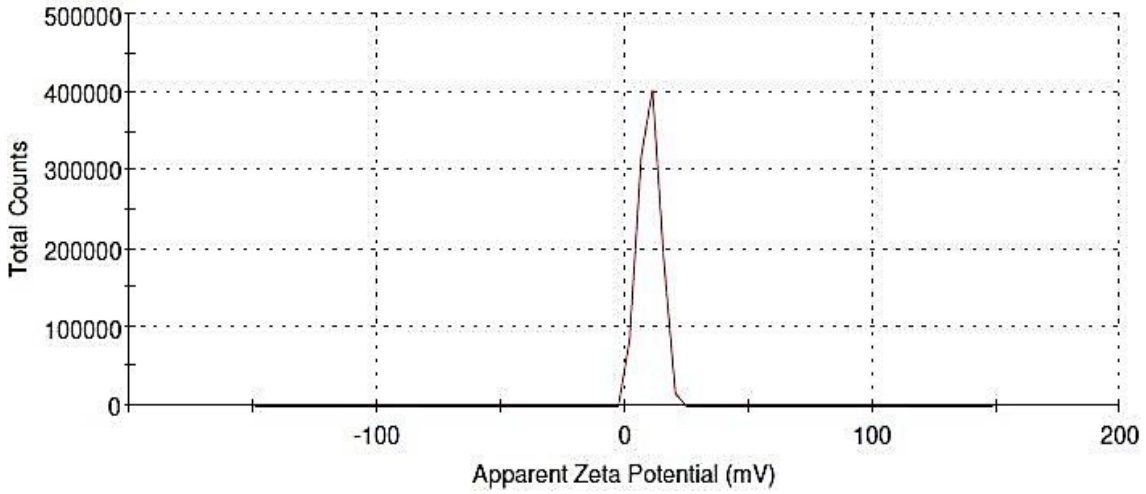


## MOF-$Al^{3+}$ 400 µL

(E)

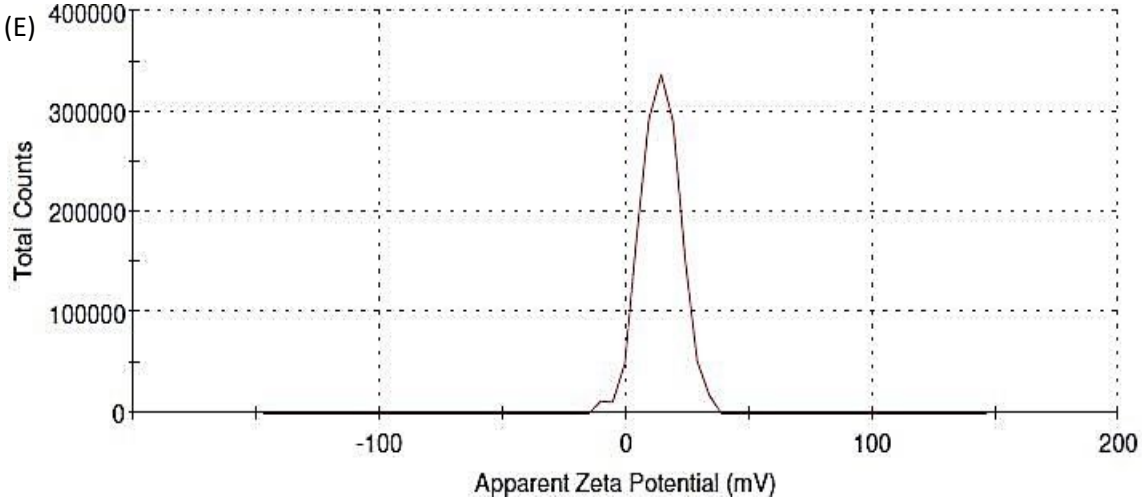


Figure 20S: The Zeta potential (DLS) of the MOF and $Al^{3+}$ solution of MOF

## 22. Effect on the UV-VIS of the MOF with addition of $Fe^{3+}$ in presence of other Metal ions

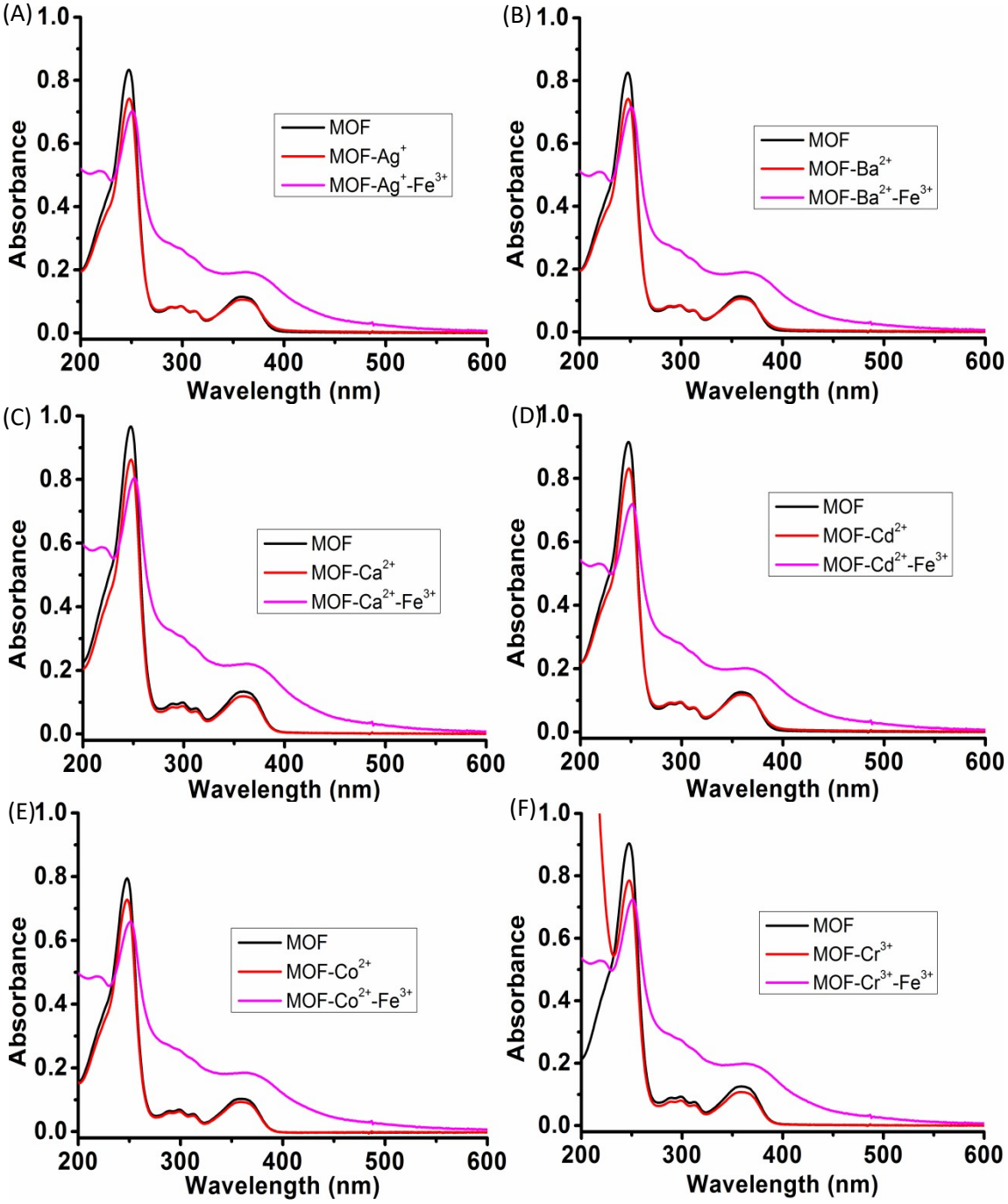

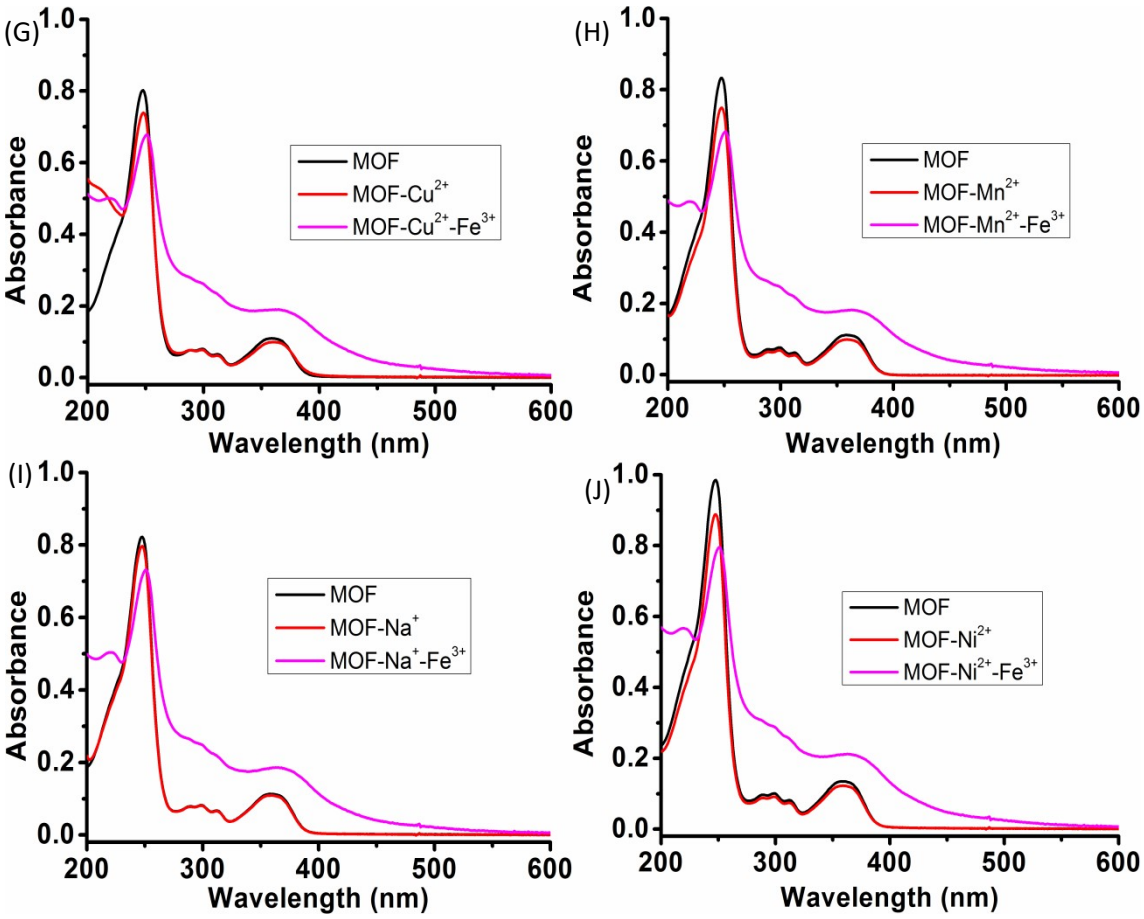


Figure 21S: Effect on UV-VIS curve nature of the MOF due to $Fe^{3+}$ addition in the MOF solution with metal ions (A) $Ag^{+}$, (B) $Ba^{2+}$, (C) $Ca^{2+}$, (D) $Cd^{2+}$, (E) $Co^{2+}$, (F) $Cr^{3+}$, (G) $Cu^{2+}$, (H) $Mn^{2+}$, (I) $Na^{+}$, (J) $Ni^{2+}$

## 23. Effect on the PL of the MOF with addition of $Fe^{3+}$ in presence of other Metal ions

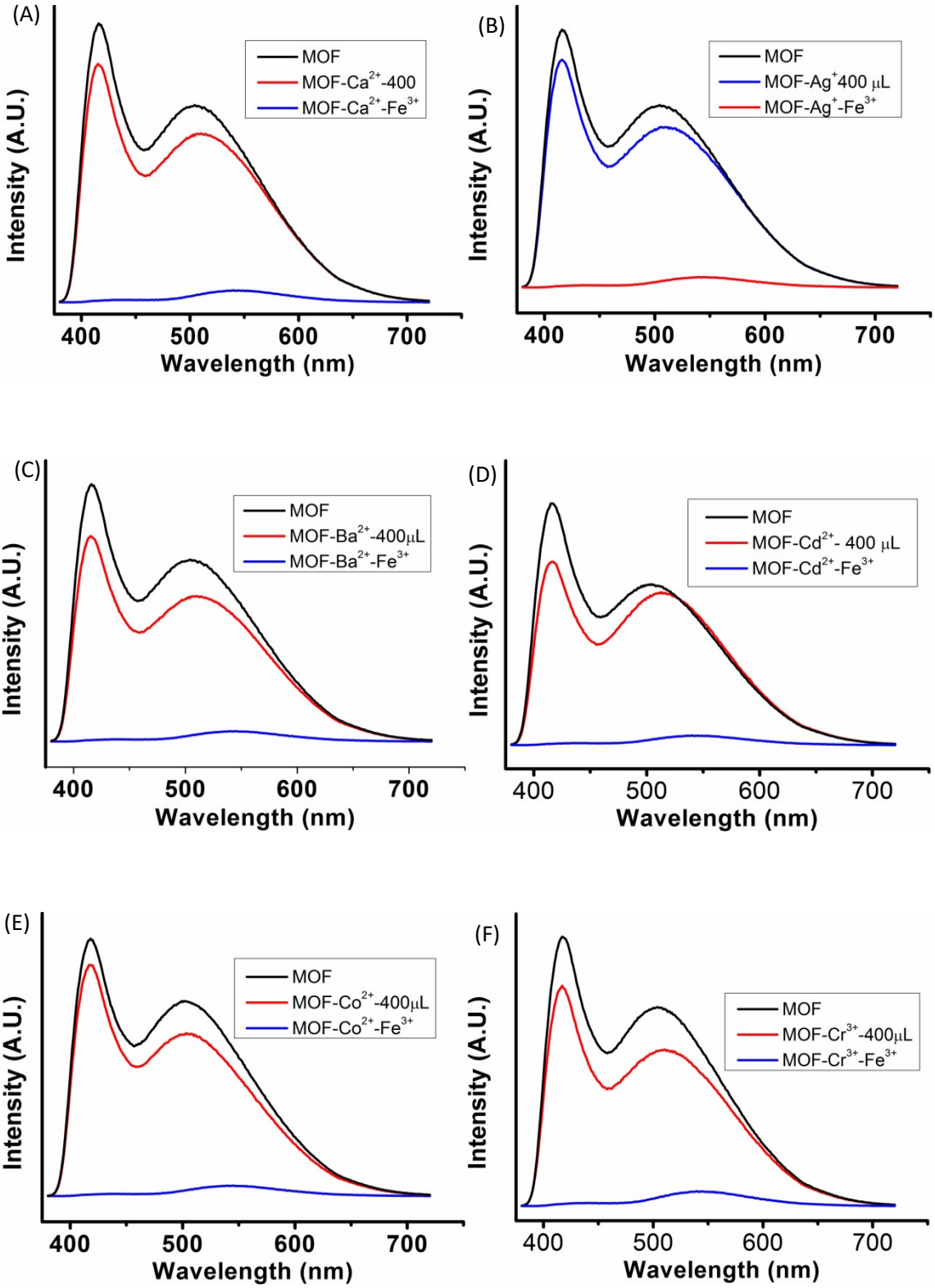

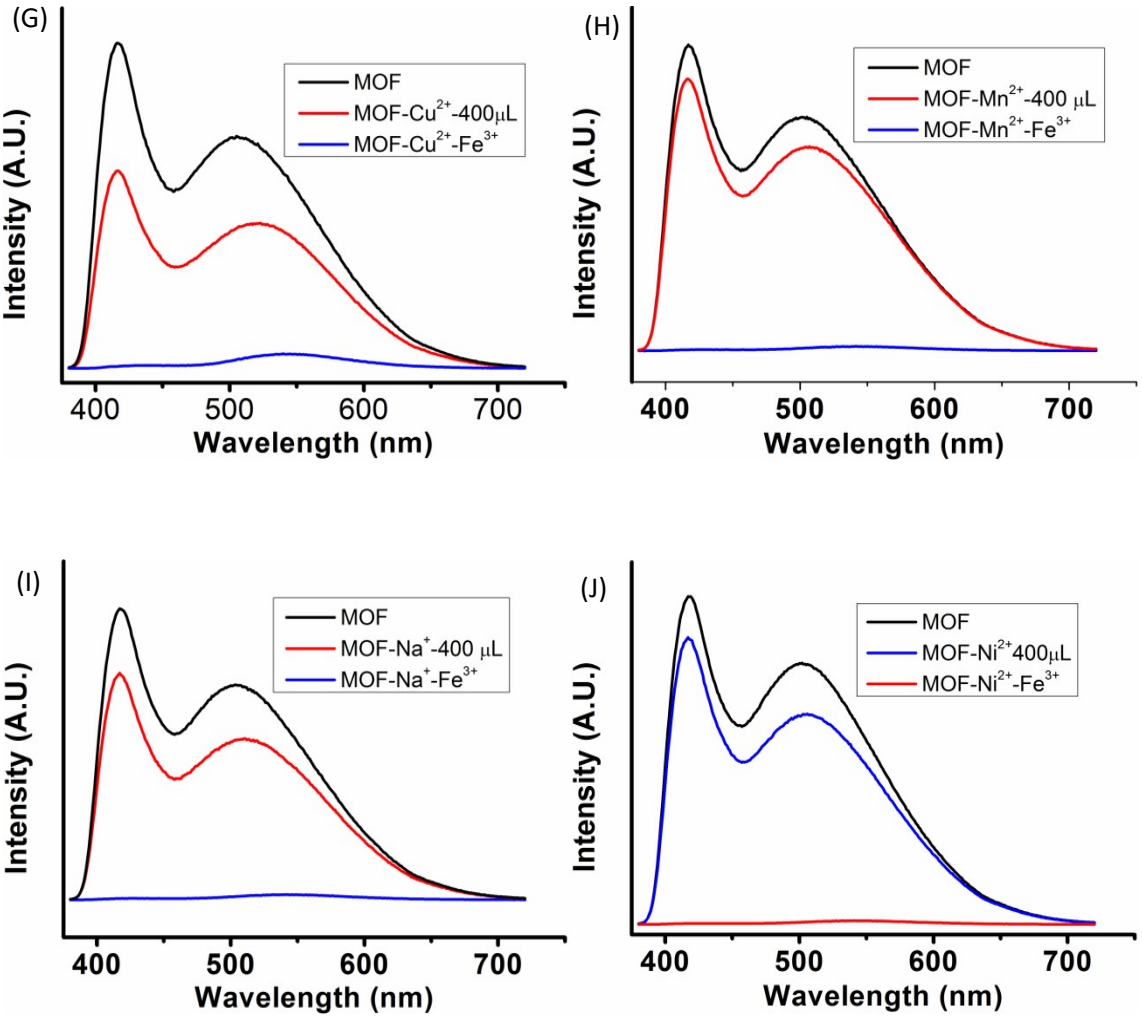


Figure 22S: Effect on PL curve nature of the MOF due to $Al^{3+}$ addition in the MOF solution with metal ions (A) $Ag^{+}$, (B) $Ba^{2+}$, (C) $Ca^{2+}$, (D) $Cd^{2+}$, (E) $Co^{2+}$, (F) $Cr^{3+}$, (G) $Cu^{2+}$, (H) $Mn^{2+}$, (I) $Na^{+}$, (J) $Ni^{2+}$

## 24. Dynamic light scattering (particle size) of the MOF in presence $Fe^{3+}$ ion

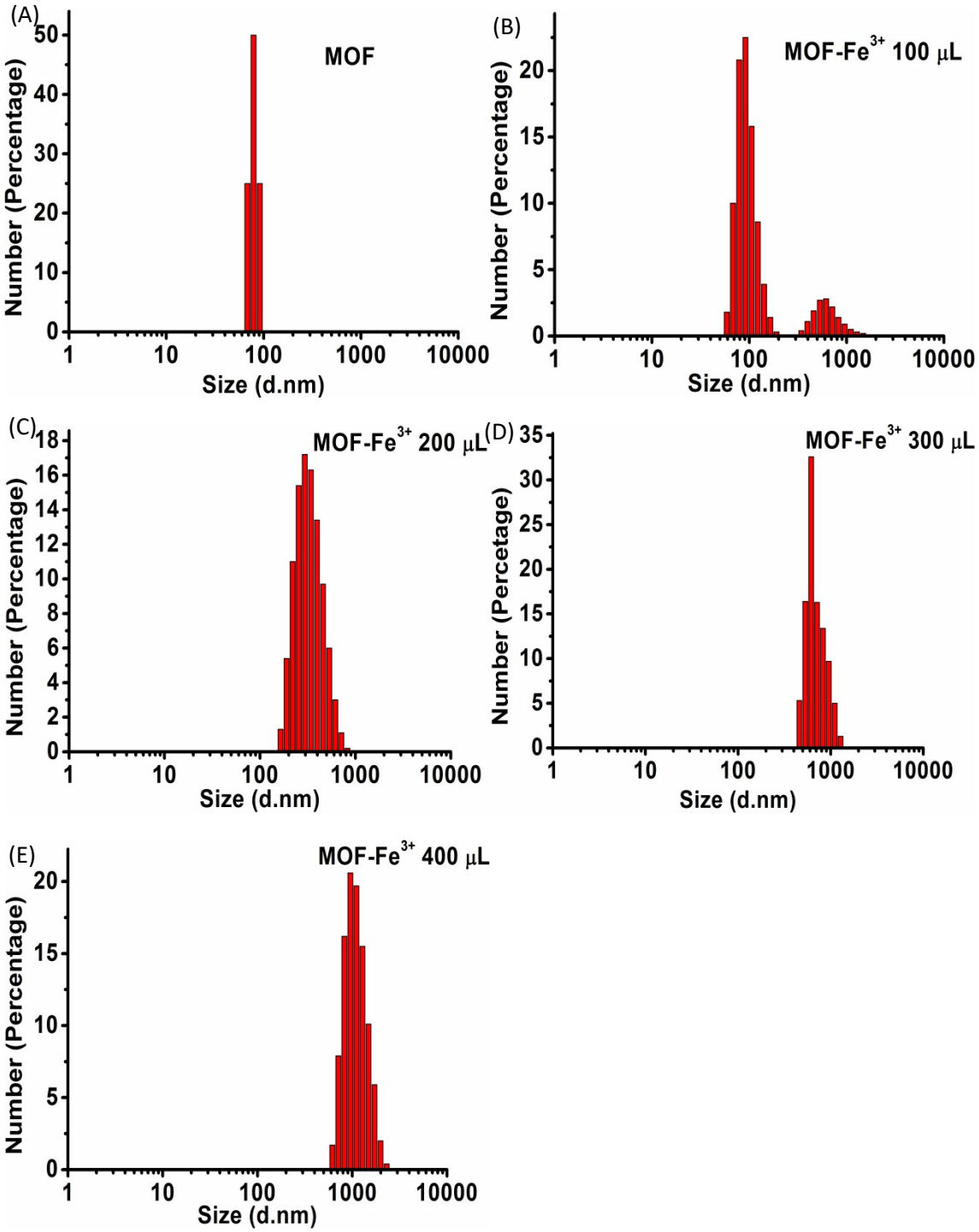


Figure 23S: The particle Size (DLS) of the MOF and MOF in presence of $Fe^{3+}$ metal ion

## 25. Zeta potential of the MOF in presence of $Fe^{3+}$ ions MOF

**MOF**

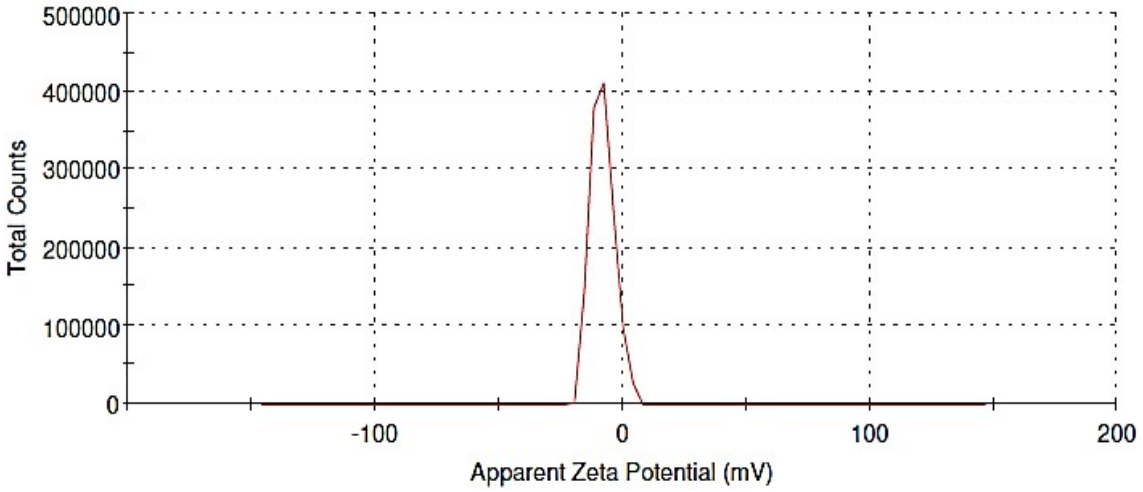


**MOF-$Fe^{3+}$ 100 µL**

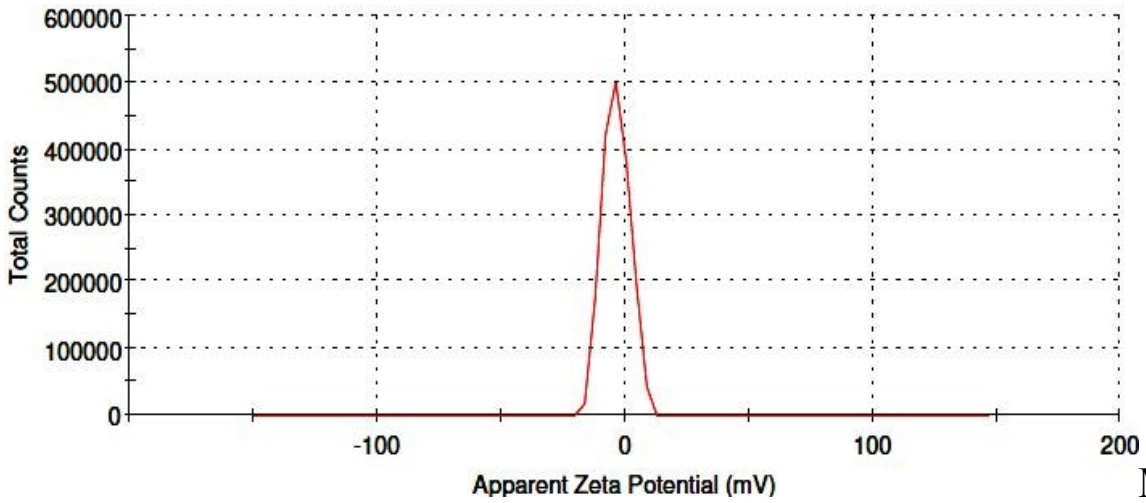


**M**

**OF-$Fe^{3+}$ 200µL**

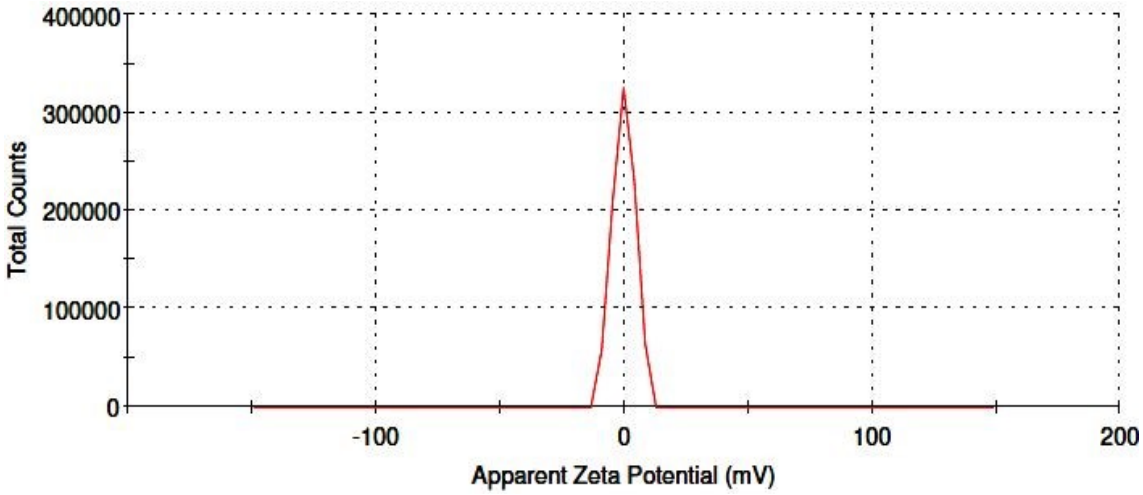

## MOF-$Fe^{3+}$ 300 µL

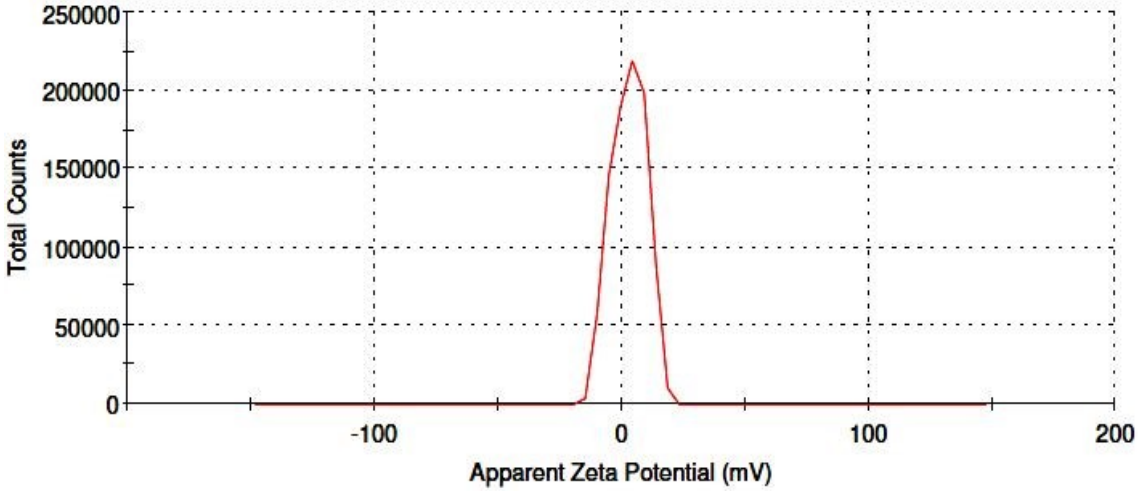


## MOF-$Fe^{3+}$ 400 µL

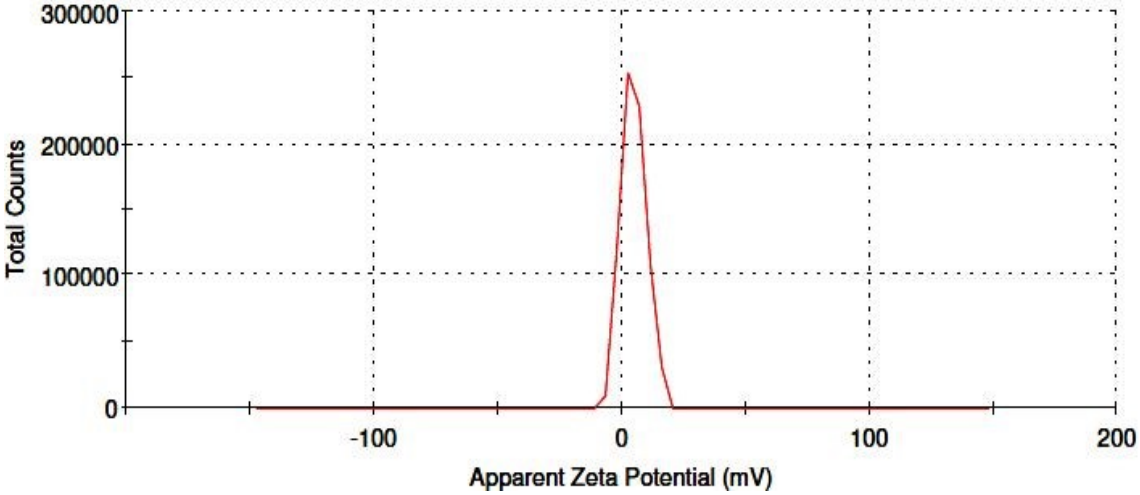


Figure 24S: The Zeta potential (DLS) of the MOF and $Fe^{3+}$ solution of MOF

## 26. Stability of MOF in different solutions

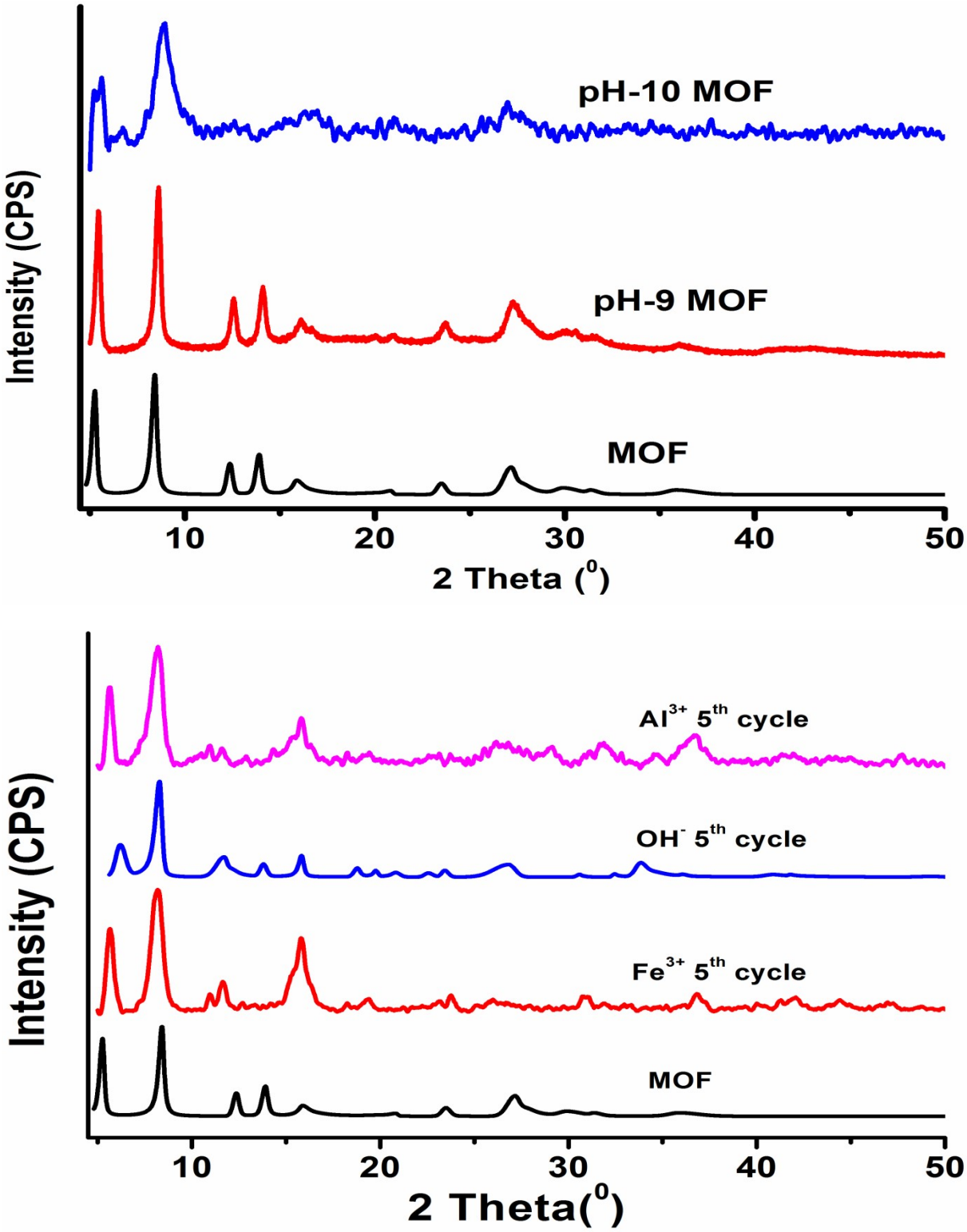


Figure 25S: PXRD of the MOF retrieved from different solution

## 27. The Stern-Volmer plot of the MOF calculated from titrations with $Al^{3+}$ and $Fe^{3+}$

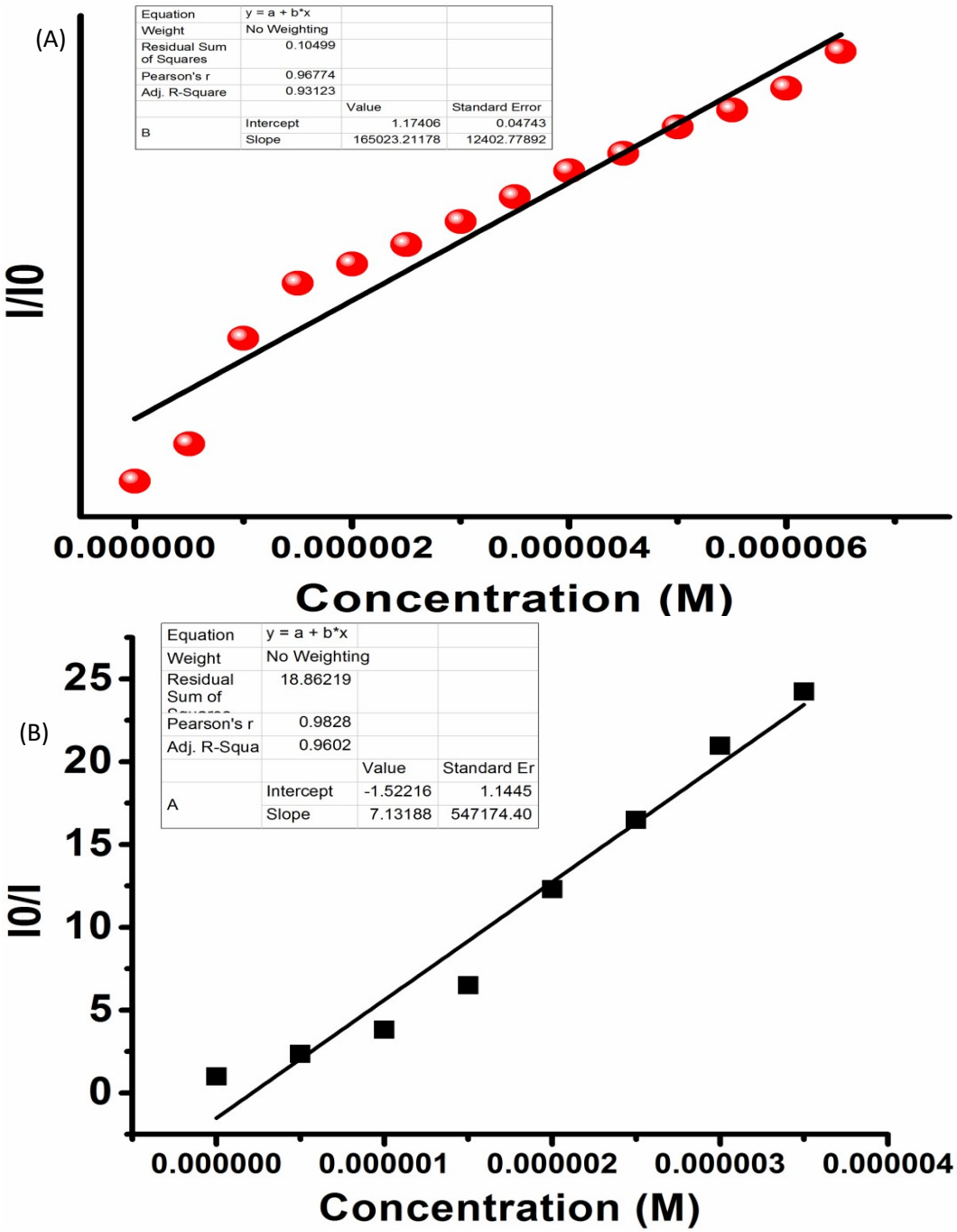


Figure 26S: (A) Represents the $K_{SV}$ plot of MOF titrated with $Al^{3+}$ solution. (B) Represents the $K_{SV}$ plot of $Fe^{3+}$ titration.

## 28. UV-VIS titration of Ligand with $OH^-$

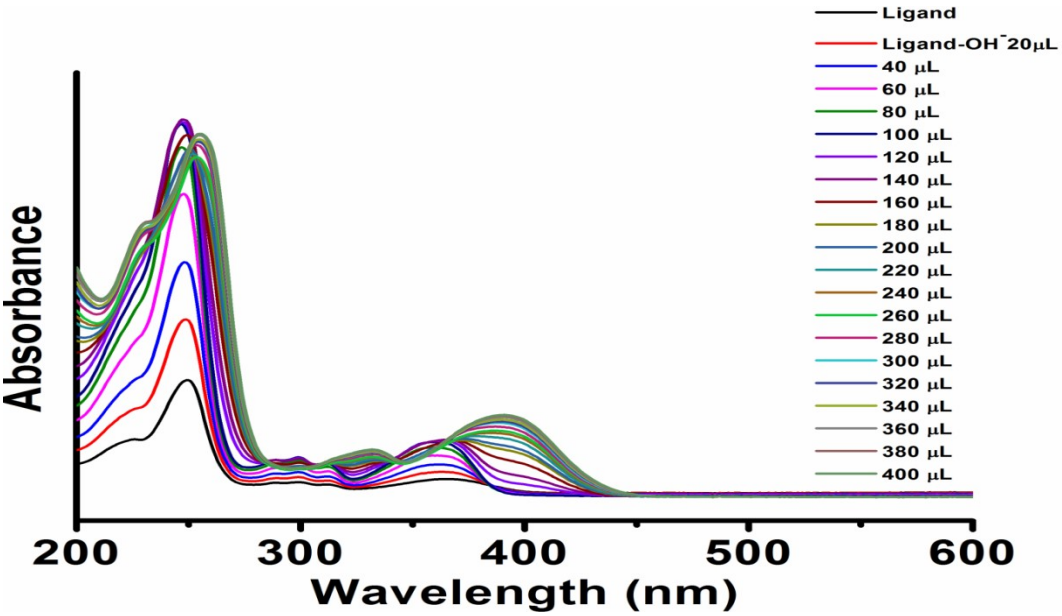


Figure 27S: The UV-VIS titration of 4, 8-dihydroxynaphthalene-2, 6-dicarboxylic acid with $OH^-$ anion.

## 29. PL titration of Ligand with $OH^-$

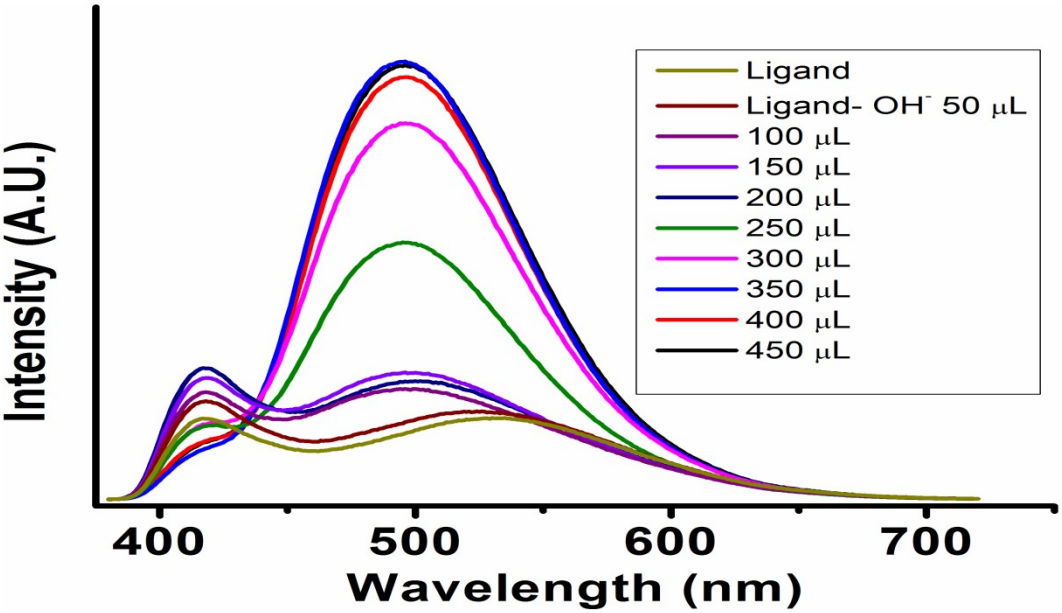


Figure 28S: The PL titration of 4, 8-dihydroxynaphthalene-2, 6-dicarboxylic acid with $OH^-$ anion.

## 30. Titration of the $Al^{3+}$@MOF with $Fe^{3+}$ ion solution

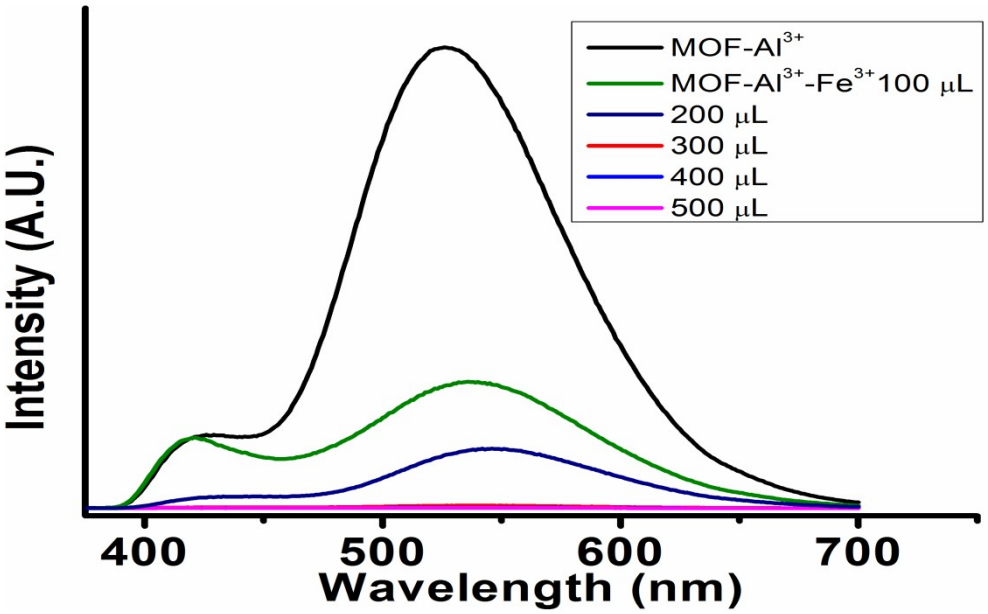


Figure 29S: The PL titration of $Al^{3+}$@MOF with $Fe^{3+}$ ions.

## 31. Titration of the $Fe^{3+}$@MOF with $Al^{3+}$ ion solution

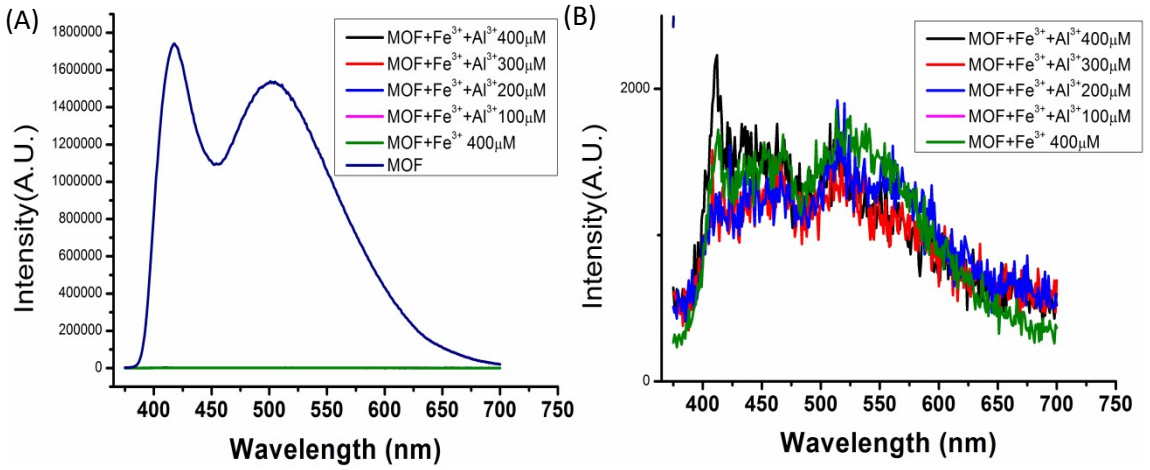


Figure 30S: The PL titration curves of $Fe^{3+}$@MOF with $Al^{3+}$ ions (A) with MOF emissions, (B) without MOF emissions.

## 32. Fluorescence Intensity of the MOF in presence of $Al^{3+}$ and calculation of LOD

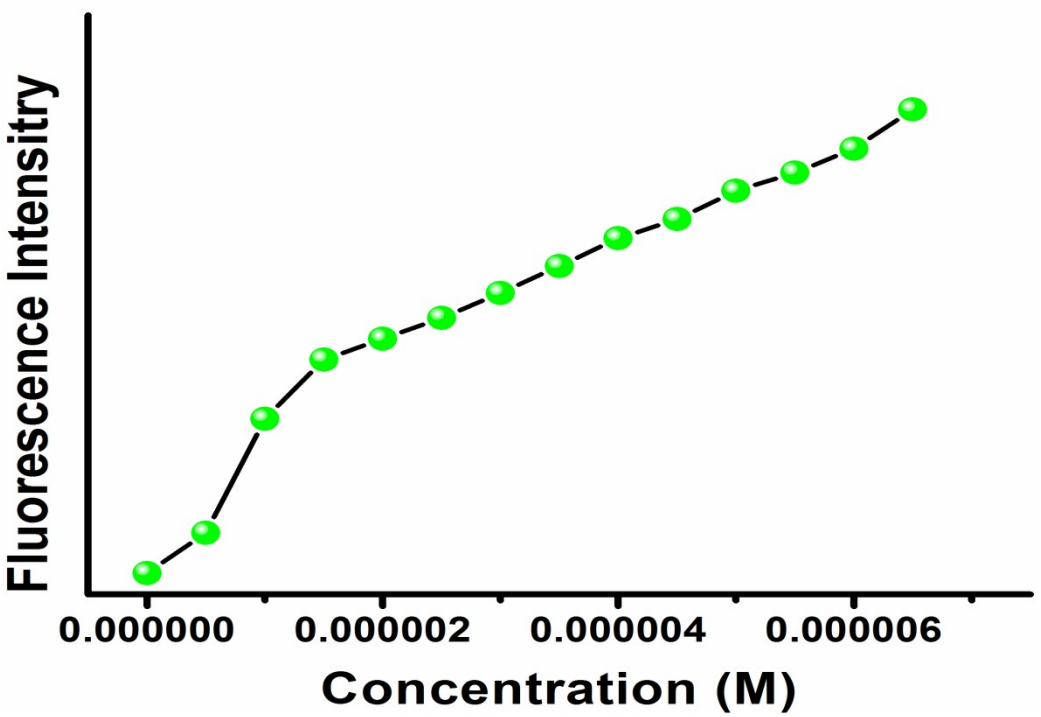


| | | | | | | | | |
|---|---|---|---|---|---|---|---|---|
| *Regression Statistics* | | | | | | | | |
| Multiple R | 0.999435054 | | | | | | | |
| R Square | 0.998870427 | | | | | | | |
| Adjusted R Square | 0.99872923 | | | | | | | |
| Standard Error | 10664.42249 | | | | | | | |
| Observations | 10 | | | | | | | |
| | | | | | | | | |
| ANOVA | | | | | | | | |
| | *df* | *SS* | *MS* | *F* | *Significance F* | | | |
| Regression | 1 | 8.04562E+11 | 8.04562E+11 | 7074.32017 | 4.4536E-13 | | | |
| Residual | 8 | 909839255.8 | 113729907 | | | | | |
| Total | 9 | 8.05472E+11 | | | | | | |
| | | | | | | | | |
| | *Coefficients* | *Standard Error* | *t Stat* | *P-value* | *Lower 95%* | *Upper 95%* | *Lower 95.0%* | *Upper 95.0%* |
| Intercept | 2163228.418 | 6268.054987 | 345.1195662 | 5.5636E-18 | 2148774.26 | 2177682.58 | 2148774.26 | 2177682.58 |
| X Variable 1 | 1.97507E+11 | 2348228547 | 84.10897794 | 4.4536E-13 | 1.9209E+11 | 2.0292E+11 | 1.9209E+11 | 2.0292E+11 |

LOD for $Al^{3+}$ is 3* standard error/co-efficient = $9.52 \times 10^{-8}$ M

Figure 31S: calculation of LOD for $Al^{3+}$ using the regression method.

## 33. Fluorescence Intensity of the MOF in presence of $Fe^{3+}$ and calculation of LOD

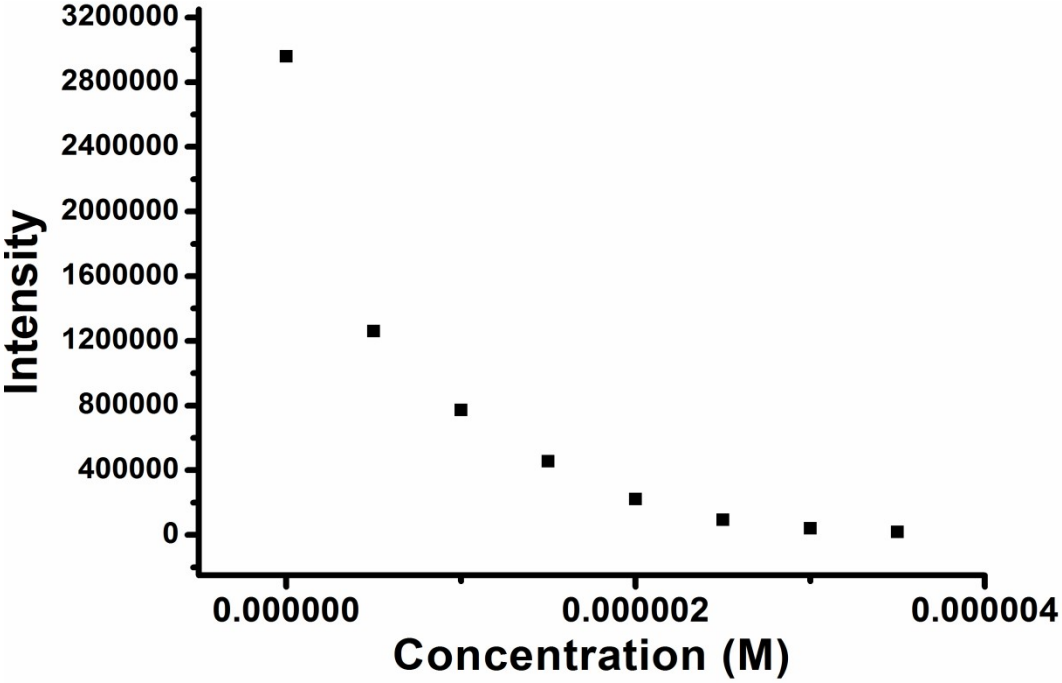


| | | | | | | | | | |
|---|---|---|---|---|---|---|---|---|---|
| SUMMARY OUTPUT | | | | | | | | | |
| | | | | | | | | | |
| *Regression Statistics* | | | | | | | | | |
| Multiple R | 0.988089032 | | | | | | | | |
| R Square | 0.976319935 | | | | | | | | |
| Adjusted R Squa | 0.96842658 | | | | | | | | |
| Standard Error | 110254.1788 | | | | | | | | |
| Observations | 5 | | | | | | | | |
| | | | | | | | | | |
| ANOVA | | | | | | | | | |
| | *df* | *SS* | *MS* | *F* | *Significance F* | | | | |
| Regression | 1 | 1.50356E+12 | 1.50356E+12 | 123.6888408 | 0.00155768 | | | | |
| Residual | 3 | 36467951859 | 12155983953 | | | | | | |
| Total | 4 | 1.54003E+12 | | | | | | | |
| | | | | | | | | | |
| | *Coefficients* | *Standard Error* | *t Stat* | *P-value* | *Lower 95%* | *Upper 95%* | *Lower 95.0%* | *Upper 95.0%* | |
| Intercept | 1669477 | 8540.519704 | 19.54833424 | 0.000292459 | 1397688.07 | 1941265.93 | 1397688.07 | 1941265.93 | |
| X Variable 1 | -7.75515E+11 | 69730865341 | -11.12154849 | 0.001557676 | -9.9743E+11 | -5.536E+11 | -9.9743E+11 | -5.536E+11 | |

LOD for $Fe^{3+}$ is 3* standard error/co-efficient = $3.3x10^{-8}$ M

Figure 32S: calculation of LOD for $Fe^{3+}$ using the regression method

## 34. Fluorescence Intensity of the MOF in presence of $OH^-$ and calculation of LOD

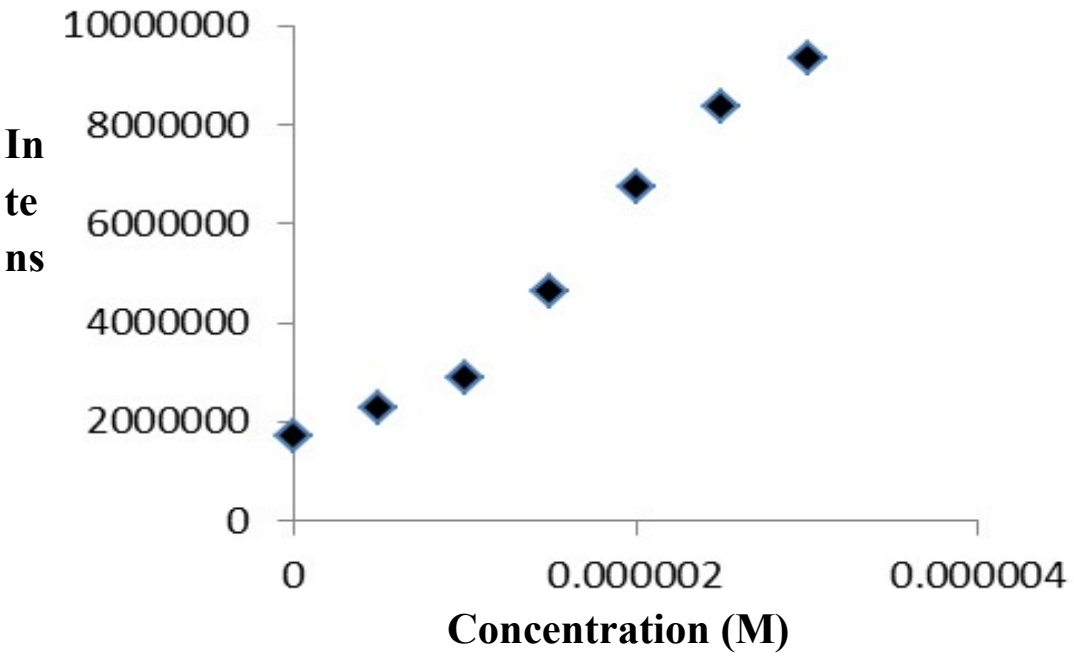


| SUMMARY OUTPUT | | | | | | | | | |
|---|---|---|---|---|---|---|---|---|---|
| *Regression Statistics* | | | | | | | | | |
| Multiple R | 0.983865948 | | | | | | | | |
| R Square | 0.967992204 | | | | | | | | |
| Adjusted R Squar | 0.961590644 | | | | | | | | |
| Standard Error | 597974.6982 | | | | | | | | |
| Observations | 7 | | | | | | | | |
| | | | | | | | | | |
| ANOVA | | | | | | | | | |
| | *df* | *SS* | *MS* | *F* | *Significance F* | | | | |
| Regression | 1 | 5.40694E+13 | 5.4069E+13 | 151.211941 | 6.2958E-05 | | | | |
| Residual | 5 | 1.78787E+12 | 3.5757E+11 | | | | | | |
| Total | 6 | 5.58573E+13 | | | | | | | |
| | | | | | | | | | |
| | *Coefficients* | *Standard Error* | *t Stat* | *P-value* | *Lower 95%* | *Upper 95%* | *.ower 95.0%* | *pper 95.0%* | |
| Intercept | 970215.5 | 40745.07574 | 2.38118282 | 0.06307248 | -77170.8342 | 2017601.834 | -77170.83 | 2017602 | |
| X Variable 1 | 2.77925E+12 | 2.26013E+11 | 12.2968265 | 6.2958E-05 | 2.1983E+12 | 3.36023E+12 | 2.198E+12 | 3.36E+12 | |

LOD for $OH^-$ is 3* standard error/co-efficient = $4.83 \times 10^{-8}$ M

Figure 33S: calculation of LOD for $OH^-$ using the regression method

## 35. Recyclability of the MOF for $Al^{3+}$, $Fe^{3+}$, $OH^-$ ions

### For $Al^{3+}$ ions

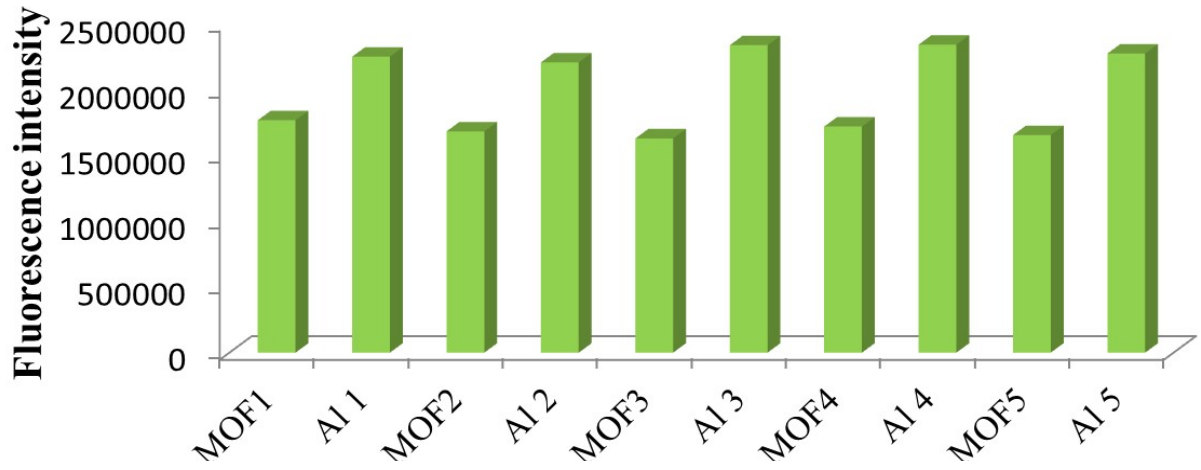


### For $Fe^{3+}$ ions

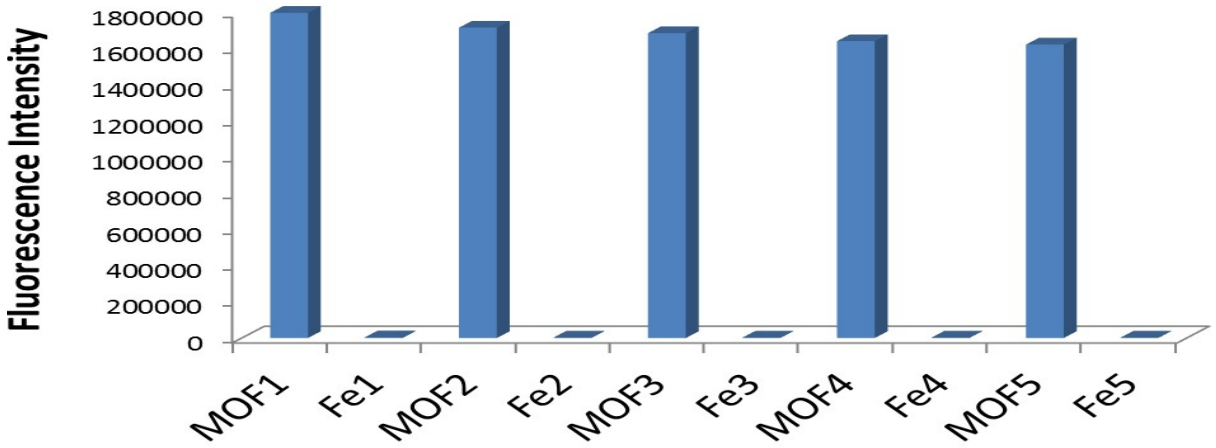


### For $OH^-$ ions

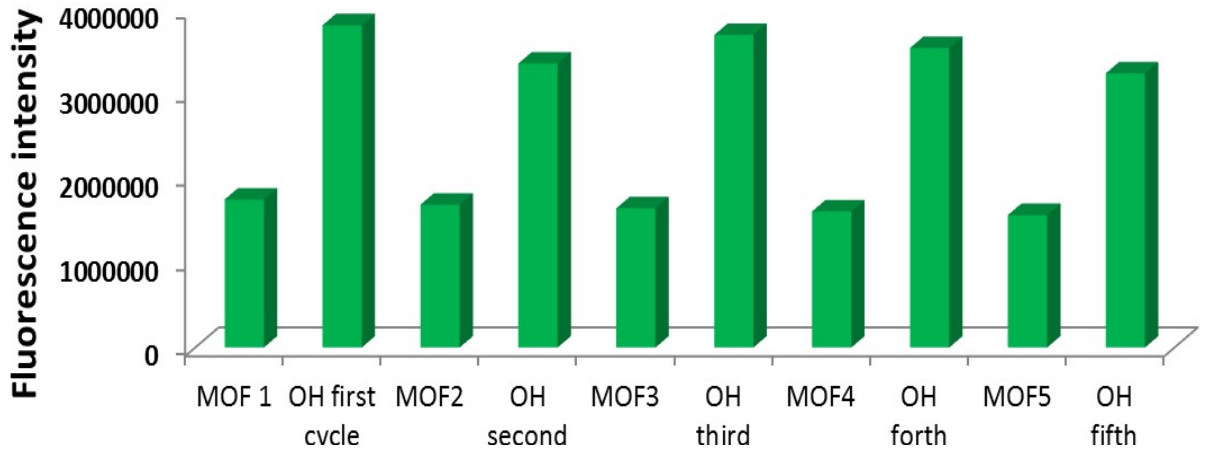


Figure 34S: The recyclability of the MOF up to 5$^{th}$ cycle for $Al^{3+}$, $Fe^{3+}$, $OH^-$ ions

## 36. Time dependent photoluminescence

### $Al^{3+}$ ions

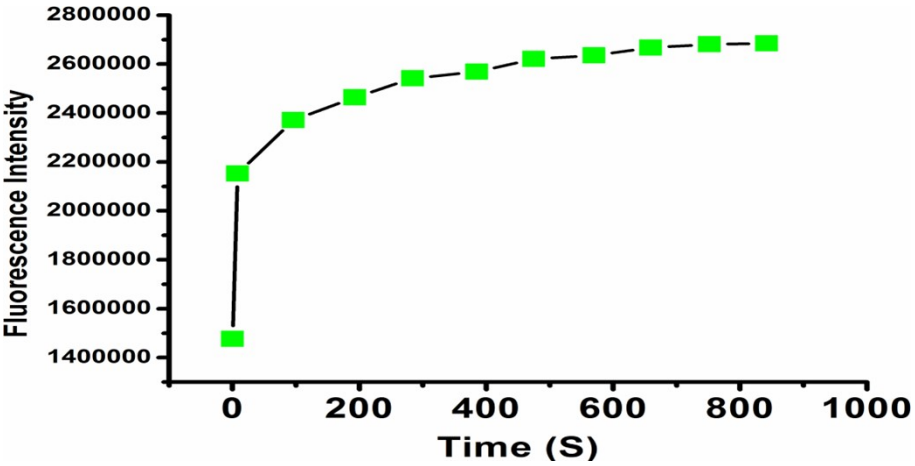


### $Fe^{3+}$ ions

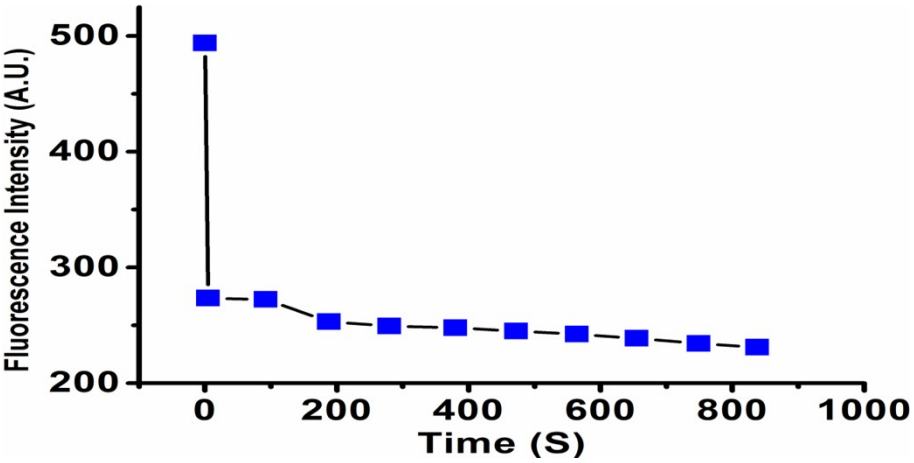


### $OH^-$ ions

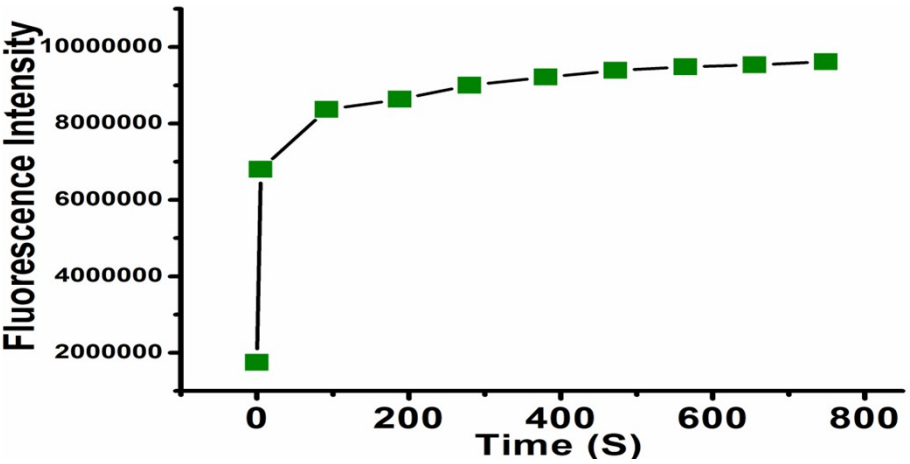


Figure 35S: the time dependent PL measuring the exposure time for $Al^{3+}$, $Fe^{3+}$, $OH^-$ ions

## 37. Zeta potential of MOF in presence of pH solutions and $OH^-$ ions

### MOF in pH-7

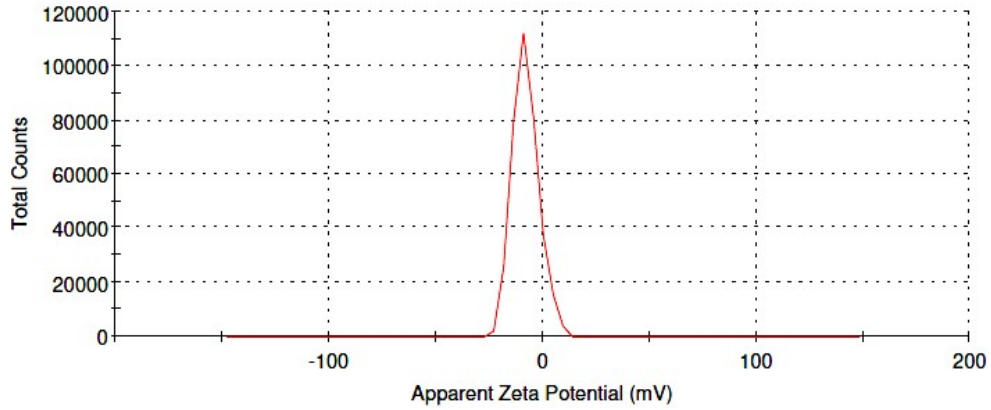


### MOF in pH-9

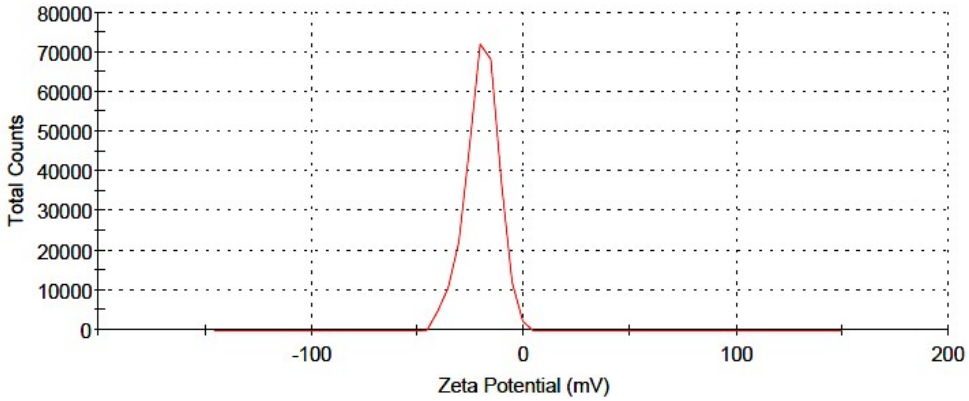


### MOF in $OH^-$ ions

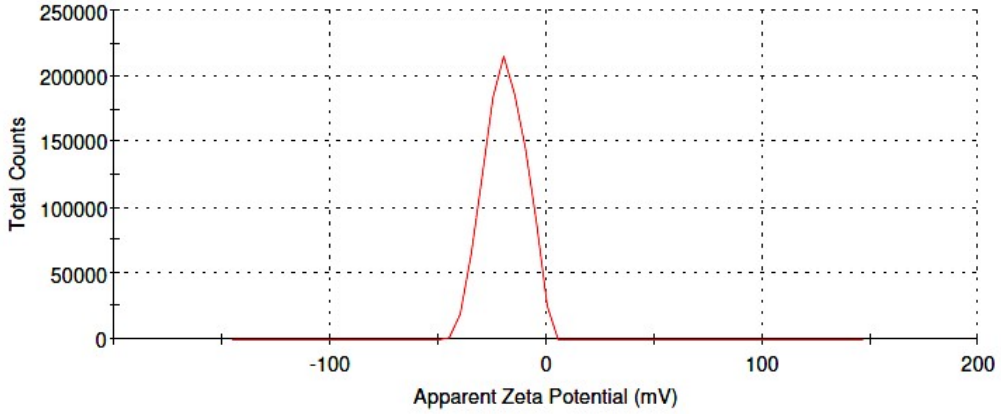


Figure 36S: Zeta potential of MOF in different pH solutions and $OH^-$ ions

# 38. EDX of MOF recovered from metal ion solution of MOF

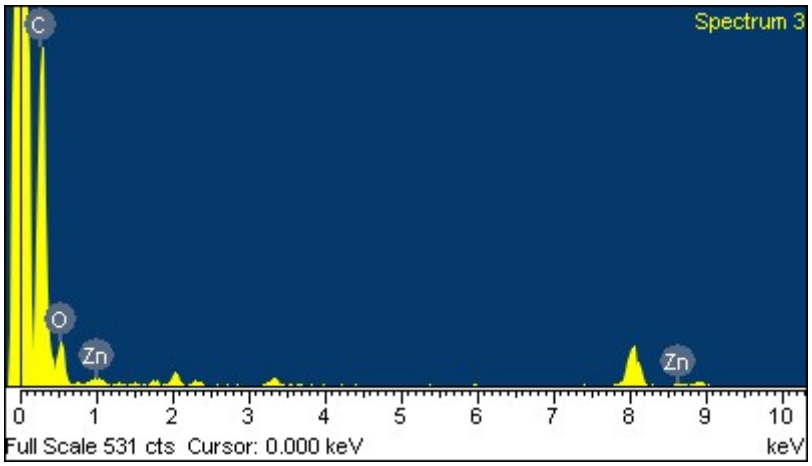


| Element | Weight% | Atomic% |
|---|---|---|
| C K | 60.01 | 62.51 |
| O K | 18.15 | 17.14 |
| Zn K | 21.84 | 20.35 |
| Totals | 100.00 | |

Figure 37S: EDX of MOF recovered from $Al^{3+}$@MOF